



AN AUTOMATED METHOD OF PREDICTING CLEAR-AIR TURBULENCE

THESIS

Brian L. Belson, Captain, USAF

AFIT/GM/ENP/04-02

**DEPARTMENT OF THE AIR FORCE
AIR UNIVERSITY**

AIR FORCE INSTITUTE OF TECHNOLOGY

Wright-Patterson Air Force Base, Ohio

APPROVED FOR PUBLIC RELEASE; DISTRIBUTION UNLIMITED

The views expressed in this thesis are those of the author and do not reflect the official policy or position of the United States Air Force, Department of Defense, or the United States Government

AFIT/GM/ENP/04-02

AN AUTOMATED METHOD OF PREDICTING CLEAR-AIR TURBULENCE

THESIS

Presented to the Faculty

Department of Engineering Physics

Graduate School of Engineering and Management

Air Force Institute of Technology

Air University

Air Education and Training Command

In Partial Fulfillment of the Requirements for the

Degree of Master of Science in Meteorology

Brian L. Belson, BS

Captain, USAF


March 2004

APPROVED FOR PUBLIC RELEASE; DISTRIBUTION UNLIMITED.

AN AUTOMATED METHOD OF PREDICTING CLEAR-AIR TURBULENCE

Brian L. Belson, BS
Captain, USAF

Approved:



Michael K. Walters (Chairperson)

27 Feb 04
Date



Ronald P. Lowther (Member)

1 Mar 04
Date



Nicole R. Benton (Member)

27 Feb 04
Date

Abstract

Clear-air turbulence (CAT) prediction is vitally important to military aviation and the successful completion of Department of Defense (DoD) operations such as air to air refueling and new national defensive weapon systems such as directed energy platforms. The unique mission requirements of military aircraft often require strict avoidance of turbulent regions. Traditionally, weather forecasters have found it difficult to accurately predict CAT. In order to forecast regions where CAT might occur, forecasters must first determine the location of breaking waves caused by either Kelvin-Helmholtz instabilities or topographically forced internal gravity waves (mountain waves) in the atmosphere. The United States Air Force (USAF) 15th Operational Weather Squadron (15th OWS) requested an updated method of predicting CAT and this request was ranked as one of the highest priority research needs by the HQ USAF Director of Weather, Deputy Chief of Staff for Air and Space Operations.

A new method of forecasting turbulence was developed in this work and the operational model was delivered to the 15th OWS for immediate inclusion into their operations. This method combines output from the Knapp-Ellrod index and the Naval Research Laboratory's Mountain Wave Forecast Model (MWFM) onto a single chart. Displaying these tools together allows forecasters to view both causes of CAT simultaneously. Furthermore, a new visualization tool is developed that allows a forecaster to view several layers at the same time as well as a composite chart to greatly reduce the time required to produce turbulence charts by OWS forecasting centers

worldwide. Tests of forecast accuracy, as determined by pilot reports (PIREPS), between charts currently produced by USAF OWSs and this new method were compared, with the new method producing far superior forecast results. This method revolutionizes the way USAF OWSs produce turbulence charts to help the Air Force satisfy each of its core competencies; especially information superiority, rapid global mobility, and precision engagement.

Acknowledgements

I would like to thank those people who most helped me complete this research. First and foremost, I thank my thesis advisor Lt Col Michael Walters for his guidance and advice throughout my research. He was the master at subtly steering me towards solutions to the problems I encountered. Also, I would like to thank the other members of my committee, Lt Col Ron Lowther and Maj Robin Benton, for the guidance in their respective areas of expertise.

In addition, I appreciate the help in implementing the Ellrod-2 index from David Knapp and Gordon Brooks at AFWA. I owe a special thanks to Earl Barker for taking his personal time to provide me with the bulk of the model data I used, without which the research would not have gone so smoothly. I also owe thanks to Dr. Steve Eckermann at NRL for his assistance with the MWFM.

Lastly, I wanted to thank my family for their help in editing this paper. To my classmates, thanks for the laughs and pretending to be interested in my thesis topic when you had your own to worry about. Thanks Capt Scott Miller, for your assistance in figuring out the MWFM. And finally, to my wife, thank you for the support and always asking, "Why aren't you done yet?"

Brian L. Belson

Table of Contents

	Page
Abstract.....	iv
Acknowledgements.....	vi
List of Figures.....	ix
List of Tables	x
I. Introduction	1
1.1 Statement of Problem.....	2
1.2 Research Objectives.....	3
1.3 Research Approach.....	3
II. Literature Review	6
2.1 Kelvin-Helmholtz Instability	6
2.1.1 Knapp-Ellrod Index	12
2.2 Mountain Waves	14
2.2.1 Mountain Wave Forecast Model V1.1	18
2.2.2 Mountain Wave Forecast Model V2.1	19
2.3 Pilot Reports.....	21
III. Methodology	24
3.1 Overview.....	24
3.2 Data.....	25
3.2.1 Model Input Data	25
3.2.2 MWFM Input Data	26
3.2.3 Ellrod 2 Input Data.....	27
3.2.4 PIREP Input Data.....	27
3.3 Index Configuration	28
3.3.1 MWFM Configuration.....	28
3.3.2 Ellrod 2 Index Configuration	31
3.4 Implementation	32
3.4.1 Index Implementation	32
3.4.2 PIREP Index Assignment Implementation	34
3.4.3 Composite Index Implementation.....	35
3.4.4 GrADS Implementation.....	35
3.4.5 Turbulence Layer Viewer Implementation	37
3.6 Statistical Methods.....	42

3.6.1 Threshold Determination	42
3.6.2 PIREP Verification	44
IV. Results.....	46
4.1 Introduction.....	46
4.2 Threshold Determination	46
4.3 Forecast Comparison	49
V. Conclusions and Recommendations	54
5.1 Conclusions.....	54
5.2 Recommendations.....	56
5.2.1 Recommendations to AFWA.....	56
5.2.2 Future Research Recommendations.....	57
Appendix A: Detailed Computations.....	60
Appendix B: CONUS what2do Script	62
Appendix C: GrADS Scripts.....	71
Appendix D: Turbulence Viewer Code	77
Appendix E: FORTRAN Code Used in Computing Indices	83
Bibliography	94
Glossary	98
Vita.....	100

List of Figures

Figure	Page
1. Contingency table used to verify turbulence forecasts	9
2. A classic model of a mountain wave	15
3. Example of output from MWFM V2.1	30
4. Example of accuracy of MWFM display using GrADS	33
5. Example composite chart.....	36
5: Example composite chart.....	37
6. Turbulence layer viewer	38
7. Examples of composite level output.....	50

List of Tables

Table	Page
1. Statistics used in index studies.....	10
2. Comparison of indices for data collected.....	11
3. Turbulence intensity threshold for Ellrod index	13
4. List of turbulence intensity values	28
5. List of flight levels based on pressure.....	39
6. Thresholds determined for indices.....	47
7. Statistics for different regions.....	49
8. Test method contingency table	51
9. OWS forecast contingency table.....	51
10. Verification statistics	52

AN AUTOMATED METHOD OF PREDICTING CLEAR-AIR TURBULENCE

I. Introduction

Over the history of aviation, atmospheric turbulence has had a huge impact on flight cost and safety. For example, turbulence cost United States commercial and military aircraft over \$25 million annually from 1963 to 1965 (Hopkins 1977). More recently, turbulence related incidents accounted for over half of all the commercial carrier accident and incident reports between the years 1990 and 2000, according to the National Transportation Safety Board (Sharman et al. 2000). Generally, there are two categories of atmospheric turbulence of concern to aviators: turbulence associated with convective clouds and turbulence that occurs outside of convective clouds. Pilots and weather forecasters are primarily concerned with turbulence occurring outside of convective clouds, or clear-air turbulence (CAT), as it rarely offers any visual indications.

CAT is defined as any turbulence in the free atmosphere of interest to aerospace operations that is not in or adjacent to visible convective activity, including turbulence found in cirrus clouds not in or adjacent to visible convective activity (Hopkins 1977). There are two widely accepted causes of CAT; either standing waves in the lee of a mountain barrier (mountain waves) or vertical wind shear in a stably stratified layer (Kelvin-Helmholtz instabilities) (Hopkins 1977). Current methods of prediction have a difficult time accurately forecasting CAT. This forecast challenge exists in part because forecasters must use synoptic scale analysis techniques and coarse resolution numerical models to predict a mesoscale phenomenon (Ellrod 1989).

1.1 Statement of Problem

Whether supporting commercial or military aircraft, forecasters spend significant time and effort predicting CAT. For example, USAF weather personnel make turbulence charts for 12, 18, 24, 30, 36, and 48 hour forecasts once per day to support United States Army and Air Force aviation. These charts should include regions of light, moderate, severe, and extreme turbulence time phased for three hours before and after the forecast hour between 10,000 and 50,000 feet mean sea level (MSL) (Air Force Manual 15-129 2001). However, in practice, most weather squadrons only forecast for moderate or greater (MOG) turbulence. The range between 10,000 and 50,000 feet is also represented as FL100-FL500. Past experience has shown these charts take significant time to prepare.

USAF weather forecasters use numerous methods, some of which are subjective, to predict CAT (15 OWS 2003). Subjective methods, such as conceptual models and rules of thumb, rely heavily on individual forecaster skill and experience, both of which vary greatly between USAF weather forecasters. Since USAF weather centers predict turbulence for large, geographically diverse portions of the earth, subjective methods are largely responsible for the substantial length of time required in building these charts.

Further increasing the time required to build turbulence charts, different methods of CAT prediction capture one cause of turbulence or the other, but not both. This limitation forces forecasters to use multiple tools while building their products. The method developed here provides a tool that displays indices representing both causes of

CAT on the same graphic, allowing the forecaster to quickly determine regions where either might occur.

1.2 Research Objectives

The primary goal of this research is to provide Air Force weather squadrons with an invaluable tool for timely and accurate prediction of CAT. Specifically, the objectives of this research are to provide USAF weather personnel with:

1. A method to quickly determine likely regions of turbulence caused by either Kelvin-Helmholtz instabilities or mountain waves;
2. An objective tool requiring little human interpretation that provides superior forecasts to those currently requiring significant human interpretation;
3. A web-based visualization tool that provides a three-dimensional, layer-by-layer view of the atmosphere; and,
4. An initial determination of the potential benefit of using the Mountain Wave Forecast Model (MWFM) to predict turbulence in the troposphere.

1.3 Research Approach

The Ellrod-2 index, as described by Ellrod and Knapp (1991), was chosen to depict Kelvin-Helmholtz instabilities. It computes a value based on vertical wind shear, horizontal deformation, and convergence. This index is built within the Operational Production System Version 2 (OPS II) software used by most OWSs. Further

substantiating its use, this index compared favorably with other indices in a study by Brown et al. (2000).

The MWFM version 1 and 2 were chosen to predict mountain waves in this study. These models were developed at the Naval Research Laboratory (NRL) to predict regions of stratospheric turbulence caused by breaking mountain waves. The MWFM is computed from atmospheric modeled data and a global ridge database. Application of the model to two case studies of tropospheric turbulence suggested it might apply there as well (Eckermann et al. 2000). In this study, both versions of the model were tested to determine if both indices added value to a forecast.

The indices were calculated over the continental United States (CONUS) using the National Center for Environmental Prediction's (NCEP) Global Forecast System (GFS) model, formerly known as the Aviation model (AVN). The MWFM retrieved the data using file transfer protocol (FTP) and stored the data locally for access by a program that computes the Ellrod-2 index. To facilitate timely completion of this research, only the analysis, 12-hour forecast, and 24-hour forecast were produced.

Initially, the output from the indices were compared with pilot reports (PIREPS), as provided by the Air Force Combat Climatology Center (AFCCC), to determine the threshold for each index. After determining the thresholds, the indices were combined into a single graphic for each 50 mb layer of the atmosphere that contained FL100-FL500 and integrated into a multiple layer viewer for forecasting. Additionally, a chart was made containing a composite view of all layers. Finally, 14 days of forecasts using these charts were developed. The accuracy of these forecasts and forecasts produced by the 15th Operational Weather Squadron (OWS) were verified against PIREPS data.

The remainder of this thesis provides details on the indices chosen and the methods used to forecast turbulence. Chapter two provides background information on the causes of CAT and the chosen indices. Then, chapter three describes the implementation of the forecast method. Chapter four discusses the results of the threshold determination and the forecast comparison. Finally, chapter five provides conclusions and suggests future research regarding this topic.

II. Literature Review

2.1 Kelvin-Helmholtz Instability

Meteorologists have long recognized and accepted breaking waves caused by Kelvin Helmholtz instabilities as a primary cause of clear-air turbulence. Kelvin-Helmholtz instabilities occur in regions of strong vertical wind shear (VWS) in stably stratified air (Hopkins 1977). Vertical wind shear is simply the change in wind speed with height while stable stratification requires more explanation.

Stably stratified air suggests relatively small vertical density differences. A modified form of the ideal gas law relates pressure, temperature, and density to each other by:

$$P = \rho RT \quad (1)$$

where P is the pressure, ρ is density, R is the dry air gas constant $287.04 \text{ J} \cdot \text{Kg}^{-1} \cdot \text{K}^{-1}$, and T is the temperature. Typically, atmospheric pressure and temperature decrease with height. Equation 1 suggests that changing pressure or temperature while holding the other constant changes the density. The equation suggests decreasing pressure causes density to decrease while decreasing temperature causes density to increase. Because the effects from decreasing pressure outweigh the effects from decreasing temperature (pressure decreases more rapidly with height), the overall effect is that density decreases with height. However, the more rapidly the temperature decreases for a given pressure decrease, the more gradual the decrease in density. Essentially, the more rapidly the temperature decreases with height the greater the stable stratification of the air.

To simplify the mathematics involved in determining the stability, potential temperature is used. Potential temperature is defined as the temperature a parcel of air would have if it were compressed or expanded adiabatically from its existing pressure and temperature to a reference pressure level (Wallace and Hobbs 1977). Basing calculations on potential temperature instead of standard temperature simplifies the determination of the stratification of the atmosphere.

Mathematically, the Richardson number (Ri) relates the two necessary conditions for Kelvin-Helmholtz instabilities as a ratio:

$$Ri = \frac{g \frac{\partial \theta}{\partial z}}{\left(\frac{\partial \bar{V}}{\partial z} \right)^2} \quad (2)$$

where g is the acceleration due to gravity, θ is the potential temperature, $\frac{\partial \theta}{\partial z}$ is the change in potential temperature with height (representing the stability of the layer), and $\frac{\partial \bar{V}}{\partial z}$ is the vertical wind shear. In order for turbulence to occur, the Richardson number must be less than a critical value of 0.25 (Thorpe 1969), which requires some combination of low static stability and high vertical wind shear. It is hypothesized that a minimum value of wind shear is required for these instabilities to form regardless of the value of the Richardson number. This implies that meeting the 0.25 threshold is a necessary, not a sufficient, condition for CAT not associated with mountain waves (Ellrod and Knapp 1991).

It is also important to note that Kelvin-Helmholtz instabilities are possible for small wavelengths, regardless of the wind shear and static stability (Ray 1986). However, small wavelengths do not cause sufficient turbulence to influence aircraft. According to Sharman et al. (2000), these waves need to be on the scale of 100 m long to affect large airframes.

Often these waves occur in air with insufficient moisture for clouds to form. When this happens they do not have any visible billow clouds associated with them. If sufficient moisture is present these waves look similar to breaking ocean waves. Like an ocean wave, the larger the amplitude of the wave prior to it breaking, the more intense the resulting turbulence.

Forecasters have relied on synoptic pattern recognition and, more recently, numerical model indices to predict these instabilities, with limited success. Both of these approaches attempt to use large scale features to determine regions that are likely to contain these relatively small scale events (Ellrod 1989). Based on the 100 m wavelength requirement, numerical model grid points would need to be spaced 10 m apart to accurately predict these waves (Sharman et al. 2000). Further limiting the effectiveness of these indices is the poor temporal resolution of both synoptic and model data. Kelvin-Helmholtz waves are short-lived (often less than 30 minutes) while synoptic and model data are typically valid every six or twelve hours.

With the introduction of computer models, researchers have recognized the usefulness of indicators other than the Richardson number to predict CAT associated with Kelvin-Helmholtz instabilities. Although a Richardson number less than 0.25 is

theoretically a good indicator of turbulent conditions, it is not well-suited to computer models for several reasons:

1. It is difficult to accurately calculate the index using a numerical model due to coarse vertical resolution (Ellrod and Knapp 1991).
2. Computations using data from rawinsondes, the best source of measurement, often lead to Richardson values between 0.25 and 1.0 in turbulent regions (Ellrod and Knapp 1991).
3. Values of Richardson less than 0.25 occur in both turbulent and smooth areas (Ellrod and Knapp 1991).
4. A detailed statistical study produced poor correlation between the Richardson number and CAT (Dutton 1980).

		Observed	
		Yes	No
Forecasted	Yes	A	B
	No	C	D

Figure 1. Contingency table used to verify turbulence forecasts

Recently, Brown et al. (2000) conducted a comparative study of 11 CAT algorithms. The 11 algorithms tested were Brown-1 (Brown 1973), Colson-Panofsky (Colson and Panofsky 1965), DTF3, DTF4, DTF5 (Marroquin 1985, 1998), Empirical

Dutton (Dutton 1980), Ellrod-1, Ellrod-2 (Ellrod and Knapp 1991), Endlich (Endlich 1964), ITFA (Sharman et al. 2000), and the Richardson number (Drazin and Reid 1981; Kronebach 1964). In Brown et al. (2000), contingency tables such as the one depicted in Figure 1 were produced for each index. In Figure 1, observed values are based on PIREPS while forecasted values are based on an index.

Table 1. Statistics used in index studies

Statistic	Definition	Description
POD _y	$A/(A+C)$	Probability of Detection of yes observations. Probability of yes observations that were correctly forecasted.
POD _n	$D/(B+D)$	Probability of detection of no observations. Probability of no observations that were correctly forecasted.
FAR	$B/(A+B)$	False Alarm Rate. Probability of yes forecasts that were incorrect.
CSI	$A/(A+B+C)$	Critical success index. Number of correct yes forecasts relative to number of yes forecasts or observations.
PC	$(A+D)/(A+B+C+D)$	Proportion correct. The proportion of yes or no forecasts that were forecasted properly.
Bias	$(A+B)/(A+C)$	Bias. Frequency of yes forecasts relative to yes observations.
HSS	$2(AD-BC)/[(A+C)(C+D)+(A+B)(B+D)]$	Heidke Skill Score. PC normalized by the number of forecasts expected to be correct.
GSS	$(A-C_2)/[(A-C_2)+B+C]$ where $C_2=(A+B)(A+C)/(A+B+C+D)$	Gilbert Skill Score. CSI corrected for the value of YY that would be expected by chance.
TSS	POD_y+POD_n-1	True Skill Score. Measure of discrimination.

Using PIREPS and automated vertical accelerometer (AVAR) observations of “g” forces, as reported by United Airlines flights, as observed values and index thresholds as forecasted values, contingency tables were produced for each index in the study. The contingency tables were used to compute the statistics described in Table 1. For reasons discussed in detail in Section 2.3, several statistics such as false alarm rate (FAR), bias,

and critical skill index (CSI) can be somewhat misleading. When considering these statistics, the probability of detection, yes and no (POD_y and POD_n) and the true skill score (TSS) are fairly reliable indicators of an index's forecast ability.

Table 2. Comparison of indices for data collected

Algorithm	Threshold	POD_y (All)	POD_y (MOG)	POD_n (PIREPs)	POD_n (AVARs)	TSS
AIRMETs	--	0.57	0.64	0.70	0.66	0.34
Brown-1	9×10^{-5}	0.58	0.62	0.63	0.58	0.25
Colson-Panofsky	-1000	0.58	0.63	0.61	0.53	0.24
DTF3	0.7	0.63	0.68	0.63	0.63	0.31
DTF4	2.5	0.63	0.67	0.57	0.60	0.24
DTF5	0.15	0.56	0.59	0.66	0.68	0.25
Empirical Dutton	25	0.62	0.66	0.57	0.57	0.23
Ellrod-1	4×10^{-7}	0.61	0.66	0.66	0.64	0.32
Ellrod-2	4×10^{-7}	0.61	0.66	0.63	0.59	0.29
Endlich	0.225	0.63	0.66	0.53	0.55	0.19
ITFA	0.13	0.57	0.62	0.67	0.65	0.29
Richardson #	4	0.58	0.63	0.66	0.64	0.29

Essentially, the reports were broken into two categories: one concerned with any turbulence and another with turbulence of moderate or greater (MOG) intensity. The results are listed in Table 2. The data used in Table 2 was adapted from Brown et al. (2000) and was collected between 21 December 1988 and 31 March 1999 for flights above 20,000 ft. Table 2 shows that DTF3, Ellrod-1 and -2 and ITFA performed the best overall. However, it is apparent the difference between POD_y values for most of the indices used in this study was relatively small. This result may be attributable to the strong similarity in the terms involved in the underlying equations for the various indices. Additionally, this table highlights the measurable improvement in skill every index experiences when predicting MOG turbulence.

2.1.1. *Knapp-Ellrod Index*. To predict turbulence caused by Kelvin-Helmholtz instabilities, Knapp and Ellrod developed two indices known as Ellrod-1 and Ellrod-2 (Ellrod and Knapp 1991). These indices are almost identical; however, because the convergence term tends to be an order of magnitude smaller than the other terms, Ellrod-1 scales it out. The indices are found by computing the product of the sum of deformation and convergence at a pressure level with vertical shear (Ellrod and Knapp 1991). The indices are derived from a version of Petterson's (1956) equation for frontogenic intensity:

$$A_T = 0.5 \left(\frac{\partial T}{\partial n} \right) (DEF(\cos 2\beta) + CVG) \quad (3)$$

$$DEF = \sqrt{DST^2 + DSH^2} \quad (4)$$

$$DST = \frac{\partial u}{\partial x} - \frac{\partial v}{\partial y} \quad (5)$$

$$DSH = \frac{\partial v}{\partial x} + \frac{\partial u}{\partial y} \quad (6)$$

$$CVG = - \left(\frac{\partial u}{\partial x} + \frac{\partial v}{\partial y} \right) \quad (7)$$

where A_T is the time rate of change of the temperature gradient on a constant pressure surface, $\frac{\partial T}{\partial n}$ is the magnitude of the temperature gradient normal to the isotherms, DEF is the square root of the sum of the squares of the stretching (DST) and shear (DSH) deformation, β is the angle between the isotherms and the axis of dilatation (stretching axis in deformation flow), and CVG is convergence. The temperature gradient term is related to vertical wind shear by the thermal wind equation:

$$\frac{dT}{dn} = \frac{fT}{g} \frac{\partial \bar{V}}{\partial z} \quad (8)$$

where f is the coriolis parameter, T is the temperature, g is the gravitational acceleration

and $\left(\frac{\partial \bar{V}}{\partial z}\right)$ is the vertical wind shear. After retaining the significant terms, equation (3)

simplifies to:

$$TI_1 = VWS(DEF) \quad (9)$$

$$TI_2 = VWS(DEF + CVG) \quad (10)$$

To determine the thresholds for the indices, Ellrod and Knapp (1991) compared forecasted events of turbulence to PIREPS. Table 3 lists the resulting thresholds. Air Force Global Weather Central (AFGWC), now known as the Air Force Weather Agency (AFWA), calculated TI_2 , or Ellrod-2, from the AFGWC global spectral model (GSM) and High-Resolution Analysis System (HIRAS). The National Meteorological Center (NMC) calculated TI_1 , or Ellrod-1, from the National Meteorological Center Nested Grid Model and Aviation Model to determine their values.

Table 3. Turbulence intensity threshold for Ellrod index

Turbulence Intensity	AFGWC	NMC NGM	NMC AVN
LGT-MDT	4		
MDT	8	4	2
MDT-SVR	12	8	4

The contingency table (see Figure 1) verification statistics at both AFGWC and NMC showed some statistical skill for several criteria. For this study, the probability of detection (POD) is the PC as outlined in Table 1. The POD was above 70% for both

AFGWC and NMC. The FAR (as described in Table 1) was 22% for the aviation model (AVN), 36% for the nested grid model (NGM) and 30-48% for AFGWC.

It is important to remember the mesoscale, short-lived nature of CAT and the relatively poor pilot report sampling of CAT identified regions when considering the high probability of false alarms. These indices predict regions where conditions are favorable for CAT to develop and not where it is actually occurring. The problem with PIREP sampling is discussed further in Section 2.3.

Additionally, in a comparative study from November 1989 to April 1990, the Ellrod Index compared well with the Empirical Dutton Index, both having similar POD and FAR (Ellrod and Knapp 1991). The Dutton index was determined using linear regression software from the University of California Los Angeles (Dutton 1980). Dutton compared PIREP data to several potential indicators of CAT including the rate of change of Richardson number (following the flow), horizontal wind shear, vertical wind shear, wind speed, vertical velocity, horizontal gradient of vertical velocity, vorticity, and deformation. Using the regression software, it determined an equation using the sum of the square of vertical wind shear and horizontal wind shear as the best predictor of turbulence.

2.2 Mountain Waves

Mountain waves have long been recognized as a cause for CAT. They typically form when the normal component of the wind to the mountain is 10 m/s or more. They are known to propagate 200km downstream of the mountain that causes them and their

intensity is usually maximized 1300m above and below the tropopause (Hopkins 1977).

Figure 2 shows a classic model of a mountain wave and areas of turbulence produced by it (Chandler 1987).

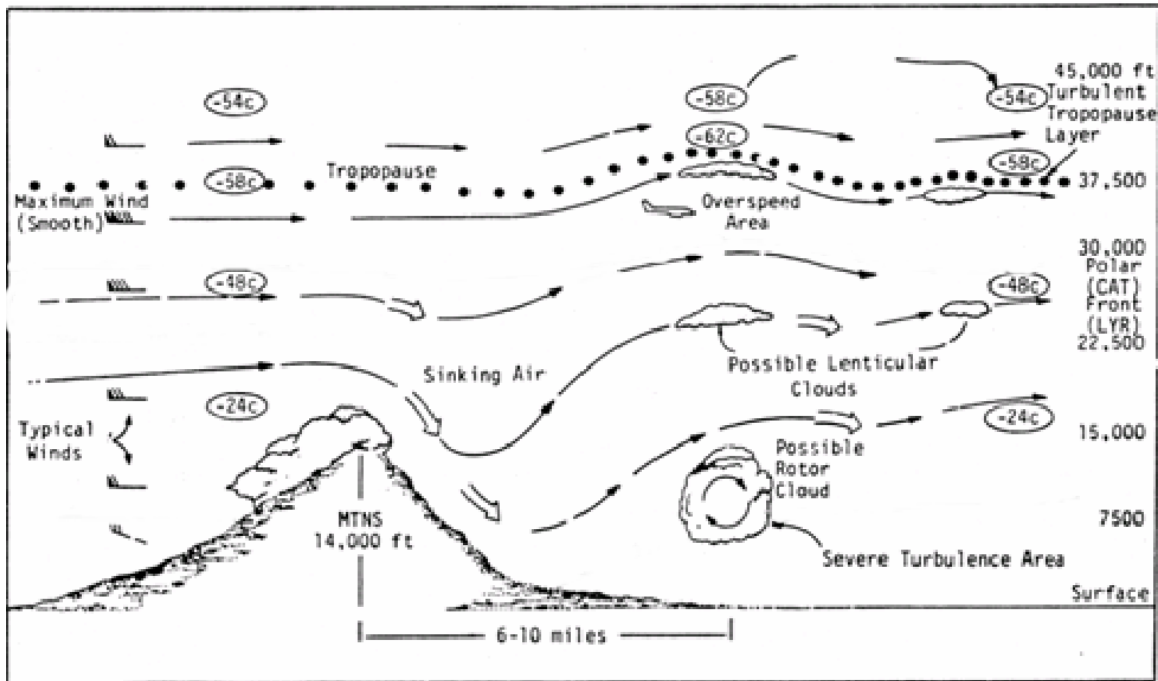


Figure 2. A classic model of a mountain wave

Mountain waves are a type of internal gravity wave. An internal gravity wave is caused by the combined force of gravity and buoyancy on a parcel of air displaced vertically (NRL 2003). When displaced, the forces of gravity and buoyancy are typically no longer in balance. This imbalance causes the parcel to accelerate vertically until it reaches a level where the forces are again in balance. In an unstable environment, an upward displaced air parcel is warmer than its surroundings. This parcel will continue to accelerate upward away from the original layer. In a stable environment, an upward

displaced air parcel is cooler than its surroundings. In this case the force of gravity is greater than buoyancy and the parcel accelerates downward toward (and beyond) its original level. This acceleration past its original level leaves it warmer than its surroundings and now the buoyancy force overcomes gravity. This causes the parcel to accelerate upward towards its original level. The situation repeats itself causing the parcel to oscillate vertically and laterally about some point in the horizontal plane (NRL 2003). In the case of mountain waves, this motion is continually forced by a mountain range.

The frequency with which the air parcel oscillates vertically is known as the Brunt-Väisälä frequency and is expressed mathematically as:

$$N^2 = \frac{g}{\theta} \frac{\partial \theta}{\partial z} \quad (11)$$

where N is the Brunt-Väisälä frequency and θ is the potential temperature. The magnitude of the Brunt-Väisälä frequency is based on the static stability of the environment. N^2 also makes up the numerator in computing the Richardson number for Kelvin-Helmholtz instabilities.

Based on the discussion in Holton (1992), the dispersion relation relates the frequency of oscillation to the wave number. This relationship determines whether the phase speed is a function of wavenumber and whether the wave pattern changes shape (disperses). In the case of topographically forced gravity waves which are stationary with respect to the ground, the dispersion relation is:

$$m^2 = \frac{N^2}{u^2} - k^2 \quad (12)$$

where m is the vertical wavenumber, \bar{u} is the mean wind flow perpendicular to the mountain range, and k is the horizontal wavenumber.

In equation 12, it is possible for m^2 to be less than zero. In this case, the waves are vertically trapped. Typically, flow over narrow ridges produces vertically trapped waves. Narrow ridges tend to cause smaller wavelengths and thus larger values of horizontal wavenumber. Additionally, small stability or a large perpendicular component of the wind might cause vertically trapped waves. In either case, vertically trapped waves typically decay exponentially with height.

When m^2 is greater than or equal to zero, the waves are vertically propagating. Vertically propagating waves occur with some combination of small mean perpendicular flow, large stability, and large horizontal wavelength. Vertically propagating waves must transport energy upward because the ground prevents downward propagation. Vertically trapped waves also propagate energy upward but the energy decays with height. Also, it is possible for both wave types to exist simultaneously (Neiman and Shaw 2003). In any case, wave energy propagates upward away from the ground, although vertically trapped wave amplitude decreases.

In the vertically propagating case, the amplitude of the wave grows with height as the air becomes less dense (NRL 2003). Occasionally, the wave breaks and turbulence results. The severity of the turbulence depends on the amplitude of the wave when it breaks. The amplitude growth with height explains why mountain wave turbulence tends to become more severe at higher altitudes.

Until recently, forecasters have relied on rules of thumb and rawinsonde observation (RAOB) data to predict the occurrence of mountain waves. When using

RAOB data, they assessed the likelihood of turbulence based on software such as the HiCAT (High Altitude CAT) analysis module which looks for “S” shaped temperature patterns in three adjacent, distinct layers and computes the parameter based on the lapse rate, mixing layer, depth of the “S” layer and the “S” layer vertical temperature difference (Sinclair and Kuhn 1991). Recently, numerical model algorithms such as the Mountain Wave Forecast Model (MWFM) have been developed and show potential for predicting mountain wave turbulence in the troposphere (Eckerman et al. 2000).

2.2.1 Mountain Wave Forecast Model V1.1. Dr. Bacmeister (1993) of the Naval Research Laboratory introduced MWFM V1.1. MWFM V1.1 calculates the distribution of mountain waves forced by air flow over a set of ridges contained in a ridge database. The ridge database was generated using a global topography dataset, compiled by the National Center for Atmospheric Research (NCAR). This dataset was used to determine ridge latitude, longitude, height, width, and orientation. MWFM V1.1 combines this information and a two-dimensional hydrostatic gravity wave model to determine the severity and extent of the waves generated by each ridge. For a detailed description of the algorithm used in determining the ridge database, refer to Bacmeister et al. (1993).

According to Bacmeister et al. (1994), MWFM V1.1 derives a turbulence estimate using the following method. First, the following assumptions are made: wave crests generated by a ridge remain parallel to the ridge, the waves generated by the flow over the ridge are hydrostatic, and the average momentum flux of the waves remains constant with height until the wave breaks. The first calculation uses the perpendicular component of the wind to each ridge to determine the stratification frequency profile over that ridge.

Next, the first guess wave displacement at each level is calculated using the following equation:

$$\delta_k^*(z + \Delta z) = \delta_k(z) \sqrt{\frac{\rho(z)N_k(z)U_{\perp;k}(z)}{\rho(z + \Delta z)N_k(z + \Delta z)U_{\perp;k}(z + \Delta z)}} \quad (13)$$

which is basically a ratio of the product of density ρ , stratification frequency N_k , and perpendicular component of the wind $U_{\perp;k}$ at two adjacent levels. If this value exceeds the saturation limit, it is reduced to equal the saturation limit. To compute the wave displacement at the surface, the minimum of the saturation limit at the surface and a multiple of the ridge height parameter is determined. The ridge height parameter is based on the deviation of the ridge height from the surrounding topography. That value is multiplied by a factor of four for the comparison.

Whenever the wave amplitude approaches or exceeds the saturation limit, some of the energy is assumed to contribute to convective and shear instability. This results in turbulence. Turbulence intensity is the difference between momentum flux computed for two adjacent levels. Momentum flux is proportional to the terms in equation 13. Due to the relatively simple, inexpensive calculations required, MWFM V1.1 is able to produce timely, world-wide forecasts for altitudes up to the mesosphere (Eckerman et al. 2000). For a more detailed look at the equations involved in calculating MWFM V1.1, refer to Appendix A.

2.2.2. Mountain Wave Forecast Model V2.1. MWFM V2.1 addressed some of the simplifications made by V1.1, at the expense of computation time, in an effort to more accurately model mountain wave dynamics. The primary changes included the

conversion from two to three dimensions and from hydrostatic to non-hydrostatic calculations. Although, the model was primarily designed for stratospheric turbulence, it has shown promise for use in the middle and upper portions of the troposphere (Eckerman et al. 2000).

According to Marks and Eckermann (1995), MWFM V2.1 is calculated using a ray tracing model. The ray tracing model tracks the trajectory and amplitude deviations of individual waves propagating through the atmosphere. In MWFM V2.1, a user-defined number of rays are launched from each ridge with a pattern that depends on the ratio of ridge width to length (Eckermann et al. 2001). In the case of a wide ridge, the rays are launched at equidistant angles from 0-180° on the downwind side of the ridge. The closer a ray is to the 90° angle, the higher the initial magnitude it is given. In the case of an isolated peak, the rays take on a pattern similar to one created by a ship's wake and the rays are assigned similar initial amplitudes. Typically, 18 rays are launched from each ridge with the MWFM V2.1.

Each ray is assigned initial values of longitude, latitude, and altitude. Additionally, the horizontal wavenumber, ground-based frequency and other terms are chosen such that the vertical group velocity is positive (Marks and Eckermann 1995). This ensures the wave energy is propagated upward. Next, the wave amplitude is determined by calculating the vertical flux of wave action. This flux is determined by multiplying the vertical group velocity and the wave action density together. The wave action density is simply the wave energy density divided by the intrinsic (Lagrangian) frequency of the wave. The vertical flux of wave action is then integrated to find the change in the vertical flux of wave action, which is used to find the wave amplitude

(Allen 2003). Once the wave amplitude is known, the calculations discussed in section 2.2.1 are applied to determine the turbulence intensity. For a detailed description of MWFM V2.1, refer to Marks and Eckermann (1995).

According to Eckermann as cited in Allen (2003), the MWFM V2.1 also accounts for the effects of friction and blocking using an arbitrary scaling factor and the local Froude number respectively. An arbitrary scaling factor accounts for friction by reducing the wind speed in the calculations. The local Froude number is the ratio of kinetic energy to potential energy. When the Froude number is on the order of one, the effective height of the terrain and the wave amplitude are reduced to account for blocking effects.

2.3 Pilot Reports

PIREPS are commonly considered the best method available for verifying turbulence forecasts. These reports are typically reported by the aircrew over the radio, but some aircraft have equipment which automatically records weather information. Aircrews typically base the intensity of the turbulence they report on their subjective interpretation while automated reports typically determine turbulence intensity by measuring the center of gravity acceleration peaks. Different sources have related different values of these peaks to different turbulence intensity. Current World Meteorological Organization (WMO) standards use the following thresholds: light ($0.15 \text{ g} \leq g^* < 0.5 \text{ g}$), moderate ($0.5 \text{ g} \leq g^* \leq 1.0 \text{ g}$), and severe ($g^* > 1.0 \text{ g}$) to quantify CAT (WMO-No. 958 2003). These values are based on g^* being the acceleration deviations

from the standard 1.0 g acceleration. The system reports turbulence measurements from these sensors as turbulence type while aircrews report turbulence intensity.

PIREPS of turbulence (or lack of turbulence) are typically entered into a 2X2 contingency table with forecasts of turbulence (or lack of turbulence) as in Figure 1. The values in these tables are then used with equations such as those listed in Table 1 to summarize the skill of a forecast method (Brown and Young 2000).

Despite being the best verification tool available, using PIREPS does pose several important problems. First, these reports frequently rely on a pilot's subjective interpretation of the severity of the turbulence encountered instead of relying on an objective, quantitative value. This may lead to inconsistencies in the reporting of CAT severity. Second, aircraft do not systematically and completely sample a grid to definitively determine the presence of CAT (Brown and Young 2000). Essentially, an aircraft usually flies a fairly direct route between two points instead of flying a grid pattern over a region. A simulation study conducted by Brown and Young (2000) demonstrates the inaccuracy in computing quantities such as FAR, bias, and other statistics when using PIREPS for CAT verification. In that study, various percentages of "yes", "no", or "yes" and "no" PIREPS were removed from a sample of 10,000 PIREPS and the various indices were recomputed. As larger percentages of PIREPS were removed, the POD_y and POD_n values remained relatively constant. However, the FAR, bias, and CSI changed significantly when a portion of either the "yes" or "no" PIREPS were removed (not both). Removal of "yes" PIREPS resulted in increased FAR, bias, and CSI while removal of "no" PIREPS resulted in decreased FAR, bias, and CSI. This suggests a strong dependence on the relative frequency of "yes" or "no" PIREPS to

the FAR (resulting from PIREP sample having different probability distribution function than the actual turbulence) and that high FAR is less significant than it might initially seem.

There are several potential problems with accelerometer data although they are more objective than PIREPS. First, depending on the size, altitude, and airspeed of the aircraft or the nature of the turbulence, the accelerometer may read different values on the accelerometer for the same turbulence encounter. Furthermore, the pilot may take actions that modify the attitude of the aircraft and cause the accelerometer value to change. These two effects limit the application of AVAR data as a tool in determining turbulence intensity.

III. Methodology

3.1 Overview

The primary goal of this research was to provide the weather forecaster with a quick, accurate method of developing turbulence charts that incorporate both primary causes of CAT. To best achieve that goal, the needs for accuracy and speed were addressed separately. This provided one distinct advantage. The speed with which the turbulence charts get developed is independent of the quality of the underlying indices. Clearly, the forecaster aids must be as skillful as possible to produce the most accurate charts. Over time, the quality and resolution of the model might improve or a superior new index might be developed. Regardless, the actual method of developing the charts does not have to change, making implementation of improvements seamless to the forecaster building the charts.

To capture turbulence caused by Kelvin-Helmholtz instabilities, the Ellrod-2 index was chosen. This index was chosen for two reasons. First, past research has identified the Ellrod-2 index as being relatively skillful in predicting turbulence (Brown et al. 2000). Second, the Ellrod-2 index is built into the software currently used by USAF weather squadrons. This allows for easy integration of this method into OWS operations.

The Mountain Wave Forecast Model was chosen to identify turbulence caused by mountain waves. As discussed previously, there are two versions of the model and for this study both versions were tested. The MWFM was chosen for two reasons also. Primarily, this model has shown some potential in predicting turbulence in the

troposphere caused by mountain waves (Eckermann et al. 2000). Additionally, the MWFM is already being implemented at AFWA to predict stratospheric turbulence. The modifications required to implement the model at tropospheric levels should be relatively easy.

The Ellrod-2 index and MWFM indices were calculated in a window from 20N-60N and 140W-30W. All but 29 of the analyses from May 20, 2003 to October 15, 2003 were used, along with PIREPS, to determine the thresholds. Additionally, the 12-hour and 24-hour forecast data were used to make forecasts from October 21, 2003 to October 27, 2003 and from November 5, 2003 to November 12, 2003. These forecasts were verified against PIREPS. Finally, 12-hour and 24-hour operational forecasts produced by USAF weather squadrons from October 21, 2003 to October 27, 2003 and from November 5, 2003 to November 12, 2003 were also verified with PIREPS.

3.2 Data

3.2.1 Model Input Data. The GFS model data were downloaded from the NCEP FTP site. The GFS model is run four times daily although this research only used the 00Z and 12Z model runs. The model also forecasts out to 120 hours. This research only looked at the analysis, 12-hour forecast, and 24-hour forecast. Horizontally, the GFS model uses spectral basis functions with resolution T254. This amounts to approximately $0.5^\circ \times 0.5^\circ$ grid point spacing in the horizontal. Vertically, the GFS model is composed of 64 sigma layers with emphasis below 800 mb and above 100 mb. This research used the layers between 800 mb and 100 mb. The data files used in this study consisted of $1^\circ \times 1^\circ$ global,

gridded model data in the gridded binary (GRIB) format. More detail on the GFS model is available at the NCEP web site (NCEP 2003). The FTP was performed by either the MWFM software or by other methods that stored the data locally. The MWFM was called from a script which first determined if the data were available locally before attempting to retrieve the data from NCEP using FTP.

The retrieved data were stored on a 36 gigabyte hard drive. To reduce the storage space required by these large data files, the data was compressed by GNU zip software available for download on-line. Compression reduced the file sizes to about 80% of their original size. This resulted in a saving of about 5 megabytes (MB) on an approximately 26 MB file retrieved from AFWA. The data stored in a local archive was retrieved from the same FTP site but the files were trimmed to include only 0-90N latitude and 180W-0 longitude instead of the entire earth. Compression on these files resulted in a savings of about 1 MB on a 5.5 MB file. Using the 5.5 MB data files required modification of the MWFM and Ellrod-2 index code to account for the different starting and ending latitude and longitude associated with those files. Finally, a third set of data files only included the necessary model fields for the necessary levels on the global grid. These files were reduced from about 10 MB to about 8 MB using compression software.

3.2.2 MWFM Input Data. The MWFM contains a variable that determines the source of the model data. Based on data availability, the “ftoption” variable was used with either a “0” option or a “2” option. The “0” option causes the model to retrieve its data locally and not to erase the data after the model run is complete. The “2” option causes the model to retrieve the data from the NCEP FTP site and not to erase the data after the

model run is complete. The MWFM used four fields from the GFS model. These include the absolute temperature, geopotential height, U wind component, and V wind component. These fields were used by the MWFM equations to calculate turbulence for every 50 millibar (mb) layer between 100 mb and 750 mb with the highest layer being the 100-150 mb layer and the lowest being the 700-750 mb layer. These layers encompass the entire section of the atmosphere necessary to produce turbulence charts from FL100 to FL500.

3.2.3 Ellrod-2 Input Data. The Ellrod-2 index was calculated using the same GFS model files used by the MWFM. The GRIB files were converted to binary files by a UNIX shell script to allow a formula translation (FORTRAN) program to read them. The shell script extracted the U wind component, V wind component, and geopotential height every 50 mb from 50-800 mb and saved each as an individual binary file. These binary files were used to calculate the Ellrod-2 index from the 750 mb level to the 150 mb level and to determine the average height over the same layers as the MWFM.

3.2.4 PIREP Input Data. A large database of military and civilian PIREPS covering the available data was received from the Air Force Combat Climatology Center (AFCCC). This database included the latitude, longitude, year, month, day, hour, altitude, and turbulence intensity fields. Unfortunately, the category (or type) of aircraft was not available in this database. As a result, all pilot report turbulence intensities were treated as if they originated from a category 2 aircraft, since weather squadron turbulence forecasts are geared towards that category of aircraft. For each model run time, any

PIREPS within a 6 hour window centered on the valid time was saved in a text file. This text file was passed to the FORTRAN program for further analysis.

This database represented turbulence intensity with a number. According to AFMAN 15-124 (2001) and WMO-No. 306 (1995) code table 0300, the number 0 corresponds to none, 1 to light, 2-5 to moderate, 6-9 to severe, and “X” to extreme. Occasional turbulence suggests turbulence occurring less than 1/3 of the time. Table 4 details the turbulence intensities as outlined in AFMAN 15-124 and WMO standards. These intensities were later scaled so that values of 0 were assigned 0, 1 were assigned 1, 2-5 were assigned 2, and 6-9 were assigned 3. All told, a sample of 18,165 PIREPS were used in this research study, of which 15,745 (May 20, 2003 – October 15, 2003) were used to set the thresholds and 2,420 (October 21, 2003 – October 27, 2003, November 5, 2003 – November 12, 2003) were used to verify the forecasts.

Table 4. List of turbulence intensity values

Value	Turbulence Intensity	Value	Turbulence Intensity
0	None	6	Occasional severe
1	Light	7	Frequent severe
2	Occasional moderate	8	Occasional severe in cloud
3	Frequent moderate	9	Frequent severe in cloud
4	Occasional moderate in cloud	X	Extreme
5	Frequent moderate in cloud		

3.3 Index Configuration

3.3.1 MWFM Configuration. For this experiment, both versions of the MWFM were tested. For both versions, the MWFM program suite is set up in modules making it easy to modify experiments for different models, locations on the earth, and regions of the

atmosphere. In this study the model was run over the entire continental United States (CONUS) from a window including 20N-60N latitude and 140W-30W longitude. This window provided diverse topography and a variety of weather conditions to test the indices.

This study initiated the MWFM from a shell script which passed the necessary date information to start the program, moved the local archive files to the appropriate MWFM data directories, chose whether to run “ftpoption” 0 or 2, moved the output to the appropriate output directory, and ensured all the necessary files were stored in the proper location. When initiated, the MWFM starts the Interactive Data Language (IDL) interface. It then immediately calls the `at_glider.pro` IDL script. This script controls the forecasting sequence by calling any necessary IDL scripts or FORTRAN programs depending on several input parameters. Most notably, the `at_glider.pro` script calls the `what2do` file which outlines the experiment and `drv_glider.pro` which calls the actual forecast routines.

The `what2do` file determines where and how the MWFM will run an experiment. It also outlines how any output will look and what parameters the program should provide to the user. It is one of several files that must be manipulated to set up a new experiment. For this experiment, the `what2do` file, `what2do_belsontest.pro`, was set up to run the model over the continental United States (CONUS) for all pressure levels that comprise the 10,000 ft to 50,000 ft MSL altitude range. The levels and field keyword were set up to reflect the desire to view the turbulence intensity variable for all the 50 millibar layers between the 800-850 mb layer and the 100-150 mb layer. The latitude and longitude limits variable was set up to cover 140W to 30W longitude and 20N to 60N

latitude. Furthermore, the what2do file was set up to run both V1.1 and V2.1 with GFS model data as input. For a copy of the what2do file used in this experiment, refer to Appendix B.

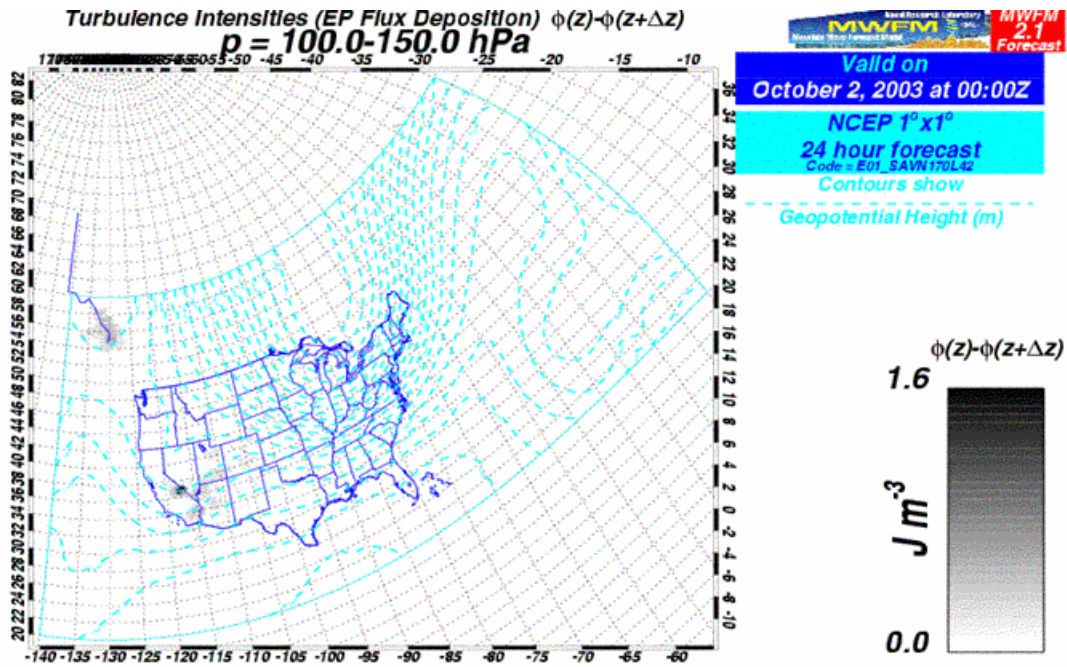


Figure 3. Example of output from MWFM V2.1

The output from MWFM V1.1 and V2.1 was set to save graphical and raw data. The graphical output was saved in postscript format. It was only used to test the accuracy of the FORTRAN code which converts the MWFM output to gridded output for display with the Grid Analysis and Display System (GrADS) software and was not configured for ideal viewing. An example of the graphical output used for testing is provided in Figure 3. In Figure 3, the dark region along the California/Nevada border indicates

turbulence. Additionally, two scripts saved the raw data with latitude, longitude, and turbulence intensity for each ridge in the window.

3.3.2 Ellrod-2 Index Configuration. The Ellrod-2 index was implemented with the same equations used in calculating the index at the Air Force Weather Agency. The equations used 2nd order centered finite differencing to compute the vertical wind shear (VWS), convergence (CVG), and deformation (DEF) terms. Using centered differencing when computing VWS introduces some error since the difference in height between pressure levels is not constant and the center pressure level is not in the geometric center. This simplification resulted in an error of 5% or less in the computation. Also, geopotential height was substituted for geometric height in the computations. According to Holton (1992), the geometric height and geopotential height are almost identical in the regions of interest for this study. Computing the index for a level requires the U and V wind data for three adjacent levels, centered on the desired level. It also required the geopotential height for the levels directly above and below the desired level. Distances were calculated using the haversine method, as described by Sinnott (1984). The equations used in the haversine method are provided in Appendix A and the FORTRAN subroutine is provided in Appendix E, subroutine Haversine. For the FORTRAN code used to compute the Ellrod-2 index, refer to Appendix E subroutine Ellrod2.

3.4 Implementation

The indices were combined using a series of shell scripts and a FORTRAN program. The controlling script retrieved the necessary analysis, 12-hour forecast, and 24-hour forecast data files (GFS U, V, and GPH fields, MWFM V1.1 and V2.1 raw data files, and PIREPS based on the date) required for the FORTRAN program. For each level, the FORTRAN program computed the Ellrod-2 index with the GFS data fields, the MWFM with the raw data, the average layer height, and the index value for each pilot report with the truncated PIREPS text file. The indices were saved to a data file for display using GrADS software while the PIREPS data was saved to a text file for statistical study.

The FORTRAN program also created another chart that provided a composite view of the indices. This chart was designed to provide the forecaster with a snapshot of the atmosphere from above that would allow them to quickly determine the horizontal location of the turbulent regions. This information was stored in the same data file as the other index files.

3.4.1 Index Implementation. The Ellrod-2 index was computed at every available level between 100 mb and 750 mb. This amounted to 14 levels separated by 50mb each. Since this computed the index for a specific level and the MWFM computed the index for a 50 mb layer, it was impossible to make the indices represent the exact same region of the atmosphere. This problem was addressed by assigning the bottom of the MWFM layer and the corresponding Ellrod-2 index to the same chart. For example, the 500-550

mb MWF layer and the 550 mb Ellrod-2 level were displayed on the same chart. The choice was made to display the Ellrod-2 index from 150 mb to 750 mb instead of from 100 mb to 700 mb since the winds at the top of the column are above the troposphere and typically do not vary as much as the winds in the troposphere.

Additionally, the average geopotential height for each layer was computed. This computation was performed for each grid point in the model by averaging the height for two adjacent levels. The results were used as the heights to assign values of each index to the PIREPS for the MWF indices. The Ellrod-2 index levels were determined using the height of the actual level for which the Ellrod-2 index was computed. The PIREPS assignment scheme is discussed further in Section 3.4.2.

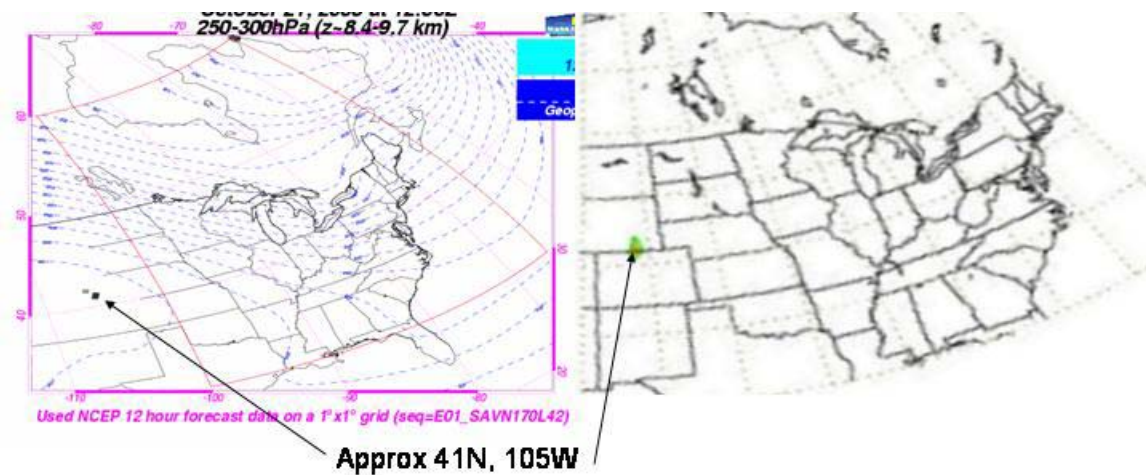


Figure 4. Example of accuracy of MWF display using GrADS

The MWF indices were computed for each grid point in the region of interest. The raw data only contained a subset of latitudes and longitudes for the region that matched ridges as contained in the MWF database. This raw data included turbulence

intensities greater than 0.0. A representative graphic on the grid was made using the largest value of the index in a 1° X 1° box centered on each grid point. This ensured that the maximum value was assigned to every point in the array, guaranteeing the worst-case is always chosen (a desirable trait where flight safety is concerned). If there were no values of raw data within that box, the grid point was assigned a value of zero. This method provided accurate results when compared to the postscript files produced by the MWFM. Figure 4 provides an example of the comparative output from the MWFM and the FORTRAN code with MWFM output on the left. The peak magnitudes for the two images in Figure 4 are located in the same place. Subroutine `Mwfm_grid` in Appendix E provides the FORTRAN code used to compute the grid point's mountain wave values.

3.4.2 PIREP Index Assignment Implementation. To calibrate the index values to turbulence intensity, pilot report data and the model analyses were used. The PIREPS were provided by AFCCC for the period of May 20, 2003 to October 15, 2003. A large file containing all the PIREPS from this period was parsed by a shell script to only include the PIREPS in a six hour window centered on the valid time of the forecast. Then, for each pilot report, the levels above and below the PIREPS were determined based on the level height for the Ellrod-2 index. Finally, the maximum of each index of the eight grid points surrounding the location of the pilot report were assigned to each PIREP. This method matched the method used in the Brown et al. (2000) study. Refer to Appendix E subroutine `PR_int` for the FORTRAN code used to assign index values to PIREPS.

3.4.3 Composite Index Implementation. The composite index was computed for all the levels and layers in the study. To determine it, the FORTRAN program computed a value of 0, 1, 2, or 3 for none, light, moderate, or severe turbulence for each grid point in the array. Turbulence values were assigned by comparing each index to each threshold, as described in Section 4.2, for every layer or level. When three adjacent layers or levels exceeded an index's threshold, and that grid point had not already been assigned a greater turbulence value, that grid point was assigned the corresponding turbulence value. For example, if the 450 mb, 500 mb, and 550 mb Ellrod-2 index values all exceeded the moderate threshold for a grid point and the grid point had previously been assigned a 0 (none) or 1 (light), the grid point was reassigned a 2 (moderate). If the same grid point had already been assigned a 3 (severe), it would have remained a 3. Refer to Appendix E, subroutine Comp_make for the FORTRAN code used to create this chart.

Additionally, the maximum value for each index for each grid point was also computed and stored in an array. Finally, these four additional fields (composite, max Ellrod-2, max MWFV V1.1, and max MWFV V2.1) were stored at the end of the data file with the individual indices for display using GrADS software.

3.4.4 GrADS Implementation. GrADS software was used to make the necessary image files for the forecaster graphics. GrADS works with unformatted FORTRAN data stored in four dimensions very easily (longitude, latitude, height, time). The data files created by this FORTRAN program saved the index values in three dimensions (longitude, latitude, height). The longitude array elements were stored from 140W-30W and the latitude array elements were stored from 20N-60N. The height elements were stored

such that the layers from 100-150 mb to 700-750 mb of the MWFM indices corresponded to the levels from 150 mb to 750 mb for the Ellrod-2 index. The composite layer was stored as an additional height layer after the bottom layer in the array. GrADS relies on metadata files to tell it how to interpret the data it reads. GrADS also has a scripting feature to string together a sequence of commands. The metadata file and script used to generate the imagery are provided in Appendix C. Information on using GrADS was obtained from on-line documentation (GrADS 2003).

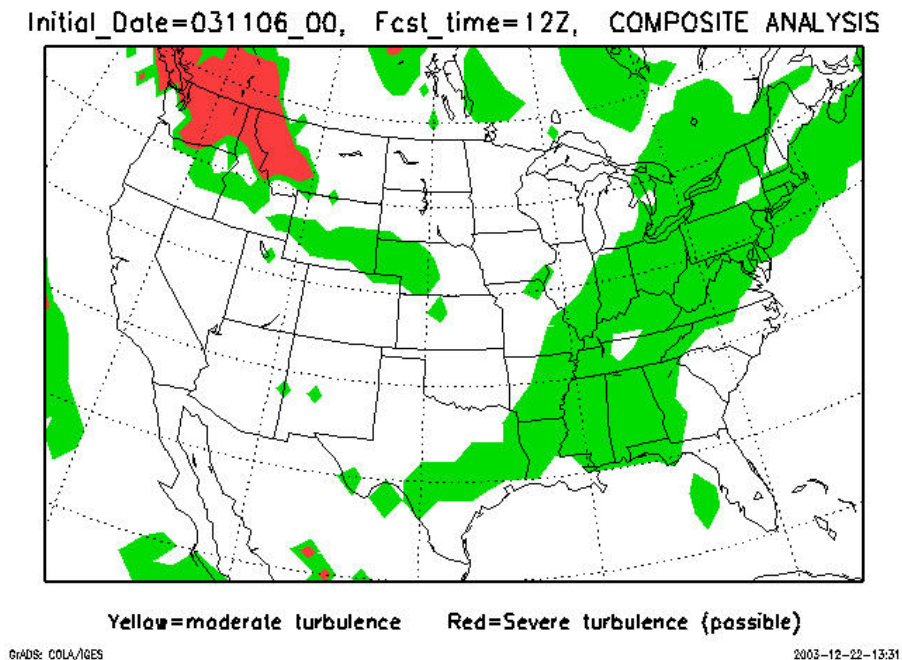


Figure 5. Example composite chart

For viewing the data, the indices were contoured on a map of the CONUS. The contours were determined by the thresholds as determined by the PIREP data. The threshold values, as determined in Section 4.2, were 2.16, 3.00, and 8.37 for the Ellrod-2

index, 0.00033, 0.00140, and undefined for MWFV V1.1 index, and 0.012, 0.020, and 0.036 for the MWFV V2.1 index. The charts developed by GrADS were saved in “Joint Photographic Experts Group” (JPEG) format.

To reduce the work required by the forecaster, a composite image was created from the composite index. This image shaded each respective threshold with values of 2 and 3 being depicted as gray shades in Figure 5. In Figure 5, regions of moderate turbulence are shaded lighter than regions of severe turbulence and are described in Section 3.4.3. The intent was to allow the forecaster to trace the regions outlined by the composite chart and use the layer viewer to determine the levels of the atmosphere that indicate the potential for CAT. This image was saved in JPEG format also.

3.4.5 Turbulence Layer Viewer Implementation. The turbulence layer viewer provided a quick method of interrogating the atmosphere and determining the turbulent levels. Because of the relatively large size an image must be to properly interrogate it with a computer, forecasters are ordinarily limited to examining each layer individually. The layer viewer circumvents that problem by allowing forecasters to view the same portion of several layers of the atmosphere at the same time.

The layer viewer requires frames and javascript to work and was designed to work with the Microsoft® Internet Explorer V6.0 web browser. It is composed of two primary areas. The first area holds the layers. To speed up the transition between layers, the viewer immediately loads all the available layers into memory despite only displaying a few of them. In this study, four layers of the 14 were displayed in the first area but that number could be easily modified. The second primary area holds the two tools needed

to control the layers. The first tool is the up/down buttons. Clicking on either of these buttons shifts the four displayed layers up or down by one layer. The other tool is a vertical scrollbar. Because of the viewing size of the four images, only a portion of each image in the first area display region is viewable at a time. Adjusting the scrollbar shifts the viewable region in each window of the first area display region to the same place. This feature may not work properly with a Netscape® browser or older Internet Explorer versions. The images used in this study did not require a horizontal scrollbar. If a horizontal scrollbar were required, a few simple modifications of the javascript used by the vertical scrollbar are all that would be required. Refer to Figure 6 for an example of the layer viewer and Appendix D for a summary of the html and javascript code used in making the layer viewer.

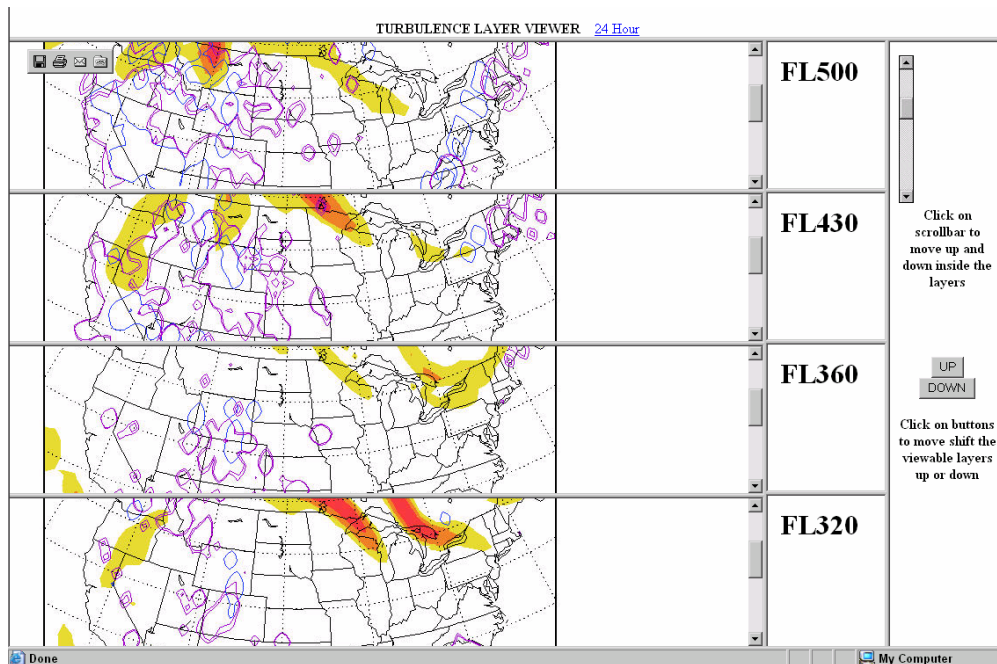


Figure 6. Turbulence layer viewer

Aside from the two primary areas, additional areas provide an approximate flight level for each layer and a title. The approximate flight level was calculated for layers below the tropopause layer using equations 14 and 15.

$$z = \frac{T_0}{\Gamma} \left[1 - \left(\frac{p}{p_0} \right)^{\frac{R_d \Gamma}{g}} \right] \quad (14)$$

$$z_{avg} = \frac{z_{layer1} + z_{layer2}}{2} \quad (15)$$

Equation 14 is based on the U.S. Standard Atmosphere below the approximate tropopause (8 km or about the 200-250 mb layer). In this equation, z is the height, R_d is the dry air gas constant $287.04 \text{ J} \cdot \text{kg}^{-1} \cdot \text{K}^{-1}$, \bar{T} is the average temperature 288.15 K, g is the acceleration due to gravity $9.80665 \text{ m} \cdot \text{s}^{-2}$, p_0 is the reference pressure 1000 mb, and p is the pressure at the level of interest. Equation 15 averages the height for the top and bottom level of each layer.

Table 5. List of flight levels based on pressure

Layer	Flight Level	Layer	Flight Level
100-150 mb	FL480	450-500 mb	FL200
150-200 mb	FL420	500-550 mb	FL170
200-250 mb	FL360	550-600 mb	FL150
250-300 mb	FL320	600-650 mb	FL130
300-350 mb	FL280	650-700 mb	FL110
350-400 mb	FL250	700-750 mb	FL090
400-450 mb	FL220		

For each of the layers, the height was verified with a sample of the model output. Additional comparison was performed visually with a skew-T of the U.S. standard

atmosphere. It is important to remember these heights are estimates of the heights in the atmosphere and are to be used as a guide. The values determined using these methods are presented in Table 5.

The region of the atmosphere chosen for the upper level turbulence charts poses a concern to this method of height determination. When flying at or above FL180, aviators set their altimeter to the standard surface pressure, 29.92 inches Hg. When flying below FL180, aviators use a nearby station pressure (FAA 2003). This difference in altimeter settings can produce differences in indicated altitude of several hundred feet. For the purpose of this study, the potential difference in altitude was considered as a possible source for error but no efforts were made to account for it since the charts assign a region of altitudes as potentially turbulent levels and not specific heights.

The data file containing the three index values and composite data was used to populate the turbulence layer viewer. The images were generated using GrADS scripts as described in section 3.4.4.

3.5 Turbulence Chart Methodology

After determining the thresholds, the test method was verified using PIREPS. Producing the turbulence charts with the test method required two steps. First, depending on the desired minimum turbulence, the contour indicating the desired turbulence intensity was outlined. For this study, MOG turbulence intensity was chosen since as a matter of practice, weather squadrons only forecast regions of moderate or greater turbulence. When two or more areas suggesting MOG turbulence were very close

together, one circle encompassing all the areas was drawn. Second, using the layer viewer, the altitudes where turbulence was present were located and the circled regions on the map were labeled with the estimated base and top of suspected turbulence. This occasionally required dividing large outlined regions into parts to make a more representative visualization.

Despite every attempt to make a purely objective forecast tool, several aspects of this method required forecaster subjectivity. First, when two or more areas on the composite chart suggesting MOG turbulence were very close together, one circle encompassing all the areas was drawn. This improved the appearance of the charts but required the forecaster to determine when two regions were close enough to be joined. Second, there were several situations that often arose when using the layer viewer which required some interpretation. First, within a layer, different intensities were present within one of the highlighted regions. In general, the level was included if more than half of the layer contained any indication of turbulence with at least some of that meeting the moderate or greater threshold. The other situation involved interpreting between two or more levels. Occasionally, two levels which obviously needed to be included were divided by a layer that appeared less likely to contain turbulence. In this instance, any indication of moderate or greater turbulence by the intermediate layer led to inclusion of that altitude. Furthermore, the top or bottom of the turbulent region rarely stopped on a layer exactly. Determining the actual heights of the top and bottom required some interpretation by the forecaster. All of the subjective decisions were made as a matter of practicality and are similar in practice to steps used by USAF weather forecasters to

estimate heights and regions of turbulence. These simplifications allow the aviators and mission planners to review a usable, easily readable turbulence chart.

Verification of charts produced by the test method and the weather squadrons were also done using the same PIREPS database. The results of both methods using the statistics discussed in Section 3.6.2 are detailed in Chapter 4.

3.6 Statistical Methods

The statistical analysis performed during this research can be divided into two primary parts. First, the thresholds for each of the three indices needed to be determined. This was done to provide a basis for the forecast tools. The primary goal of this stage was to determine usable values of each index that correspond with light, moderate, and severe turbulence. These thresholds were then used to create the images used by the turbulence viewer software to assist the forecaster in turbulence chart development. The second stage of the statistical analysis involved verifying forecasts produced using the test method with PIREPS and comparing it to verification of actual forecasts produced by USAF weather squadrons.

3.6.1 Threshold Determination. The thresholds were determined with a FORTRAN program which processed every possible combination of indices looking for the ideal combination based on contingency table statistics as described in Table 1. Several different criterion were compared to determine the thresholds including the PODy maximum, PODn maximum, FAR minimum, CSI maximum, PC maximum, TSS

maximum, closest BIAS score to one, the first instance when POD_y was less than or equal to POD_n, the maximum HSS, and the maximum GSS.

The HSS and GSS are statistics developed to determine the actual skill of a forecast relative to random forecasts. According to Wilks (1995), the HSS is the most common skill score used to summarize square contingency tables. It essentially compares the forecasts to a generic reference forecast, using the equation in Table 1, with the same marginal distributions of forecasts and observations as the actual contingency table. The HSS returns a value less than or equal to one. A score of one signifies a perfect forecast while forecasts worse than the generic reference forecast receive scores less than zero. Schaefer (1990), describes the GSS as the CSI corrected for the number of hits expected by chance. A perfect forecast receives a score of one. The closer a forecast is to being purely random, the closer the GSS will be to zero (Stephenson 2000). The equations used in calculating the HSS and GSS are listed in Table 1.

The FORTRAN program contained four nested loops. The loops cycled through every combination of the three indices over user-determined ranges of values at user-determined increments. Additionally, the program could be configured to analyze different flight levels, turbulence intensities, latitude/longitude ranges, and different lengths of time centered on the forecast hour for the same statistics. After computing the statistics, the FORTRAN program saved the results to an output file for review.

After determining the thresholds, the χ^2 test, as described in Montgomery and Runger (2003), was performed on the contingency tables to test for independence. In this test, the null hypothesis was that forecasts were independent of observations. An alpha of 0.05 was used to reject the null hypothesis and determine whether forecasts and

observations of turbulence were dependent on each other. The test statistic in a χ^2 test is computed using the equation:

$$\chi^2 = \sum_i \sum_j \frac{(O_{ij} - E_{ij})^2}{E_{ij}} \quad (16)$$

where O_{ij} is the observed contingency table values, E_{ij} is the expected table values, and i and j are the rows and columns. The observed contingency table is the contingency table calculated from the data while the expected contingency table is computed using:

$$E_{ij} = \frac{tot_i(tot_j)}{total} \quad (17)$$

where tot_i represents the total of row i in the observed contingency table, tot_j is the total of column j in the observed contingency table, and $total$ is the sum of all the cells in the observed contingency table. After determining the χ^2 value for the data, it was compared to the table value of χ^2 for an alpha of 0.05 with 1 degree of freedom or 3.84. If the computed χ^2 value exceeded 3.84, the null hypothesis was rejected.

3.6.2 PIREP Verification. After the thresholds were determined, the layer viewer software was configured with the thresholds to allow for forecasts to be developed. These forecasts were made over the CONUS from October 21, 2003 to October 27, 2003 and from November 5, 2003 to November 11, 2003. Contingency tables combining PIREPS and forecasts were used to compute the same statistics discussed in section 3.6.1. Additionally, forecasts produced by USAF weather squadrons over the CONUS for the same dates were verified using the same methods. The USAF weather squadron forecasts originated from stitched charts produced by the 26th OWS at Barksdale AFB. These

stitched charts represented the combined forecasts of turbulence charts produced by the 15th OWS at Scott AFB, 25th OWS at Davis-Monthan AFB, 26th OWS at Barksdale AFB, and 28th OWS at Shaw AFB.

IV. Results

4.1. Introduction

This chapter summarizes the results from the various contingency table analyses performed using the PIREPS and the various forecasts. It begins with a discussion of the various analyses performed on the data to determine the different thresholds. This includes testing for whether the thresholds vary by altitude or geographic region. It also includes testing the thresholds for turbulence greater than or equal to light, greater than or equal to moderate, and greater than or equal to severe. After completing the threshold determination, the established thresholds were entered into the FORTRAN program that computed the indices and the program was rerun to generate the products used by the test forecast method. The second section describes the results of the forecast comparison between the test method and operational forecasts. It focuses on the relative accuracy of the test method to the forecasts currently produced by the various weather squadrons.

4.2. Threshold Determination

Thresholds were determined using the subset of PIREPS within six hours of the model analysis runs from May 20, 2003 to October 15, 2003. For example, for a model forecast valid at 12Z, any PIREP between 0900 and 1459 were used. Using this subset of PIREPS provided a sample size of 15,745. In determining the thresholds, the Ellrod-2 index threshold was found for each intensity level first. This was done by setting the

ranges for the MWFM indices with a value of 99.0. This value was well outside of maximum value of either MWFM index. After determining this threshold, the MWFM V2.1 threshold was found with the Ellrod-2 index set to its already determined threshold. Finally, the MWFM V1.1 threshold was found with the other two indices set to their established thresholds. This order of threshold determination was chosen because the MWFM V1.1 threshold tends to contain output for the region directly above a ridge while MWFM V2.1 propagates energy downstream making it provide output over larger regions of the map. The order intended to ensure the best chance that each index contributed to finding positive reports of turbulence the other indices, covering larger areas, missed. The criteria most often used to set the thresholds included the skill scores and the point where PODy crossed PODn. The results of threshold determination are provided in Table 6.

Table 6. Thresholds determined for indices

		Light			Moderate			Severe		
Chart	Index	TH	PODy	PODn	TH	PODy	PODn	TH	PODy	PODn
Layers	Ellrod 2	2.16	0.50	0.63	3.00	0.45	0.67	8.37	0.21	0.94
	MWFM V1	0.00033	0.67	0.49	0.0014	0.56	0.60	-	-	-
	MWFM V2	0.012	0.66	0.49	0.02000	0.54	0.61	0.03600	0.33	0.87

From Table 6, the light and moderate thresholds were quite close to each other for each of the indices. This would make separating regions of light and moderate turbulence difficult. Since Air Force weather squadrons only predict regions of moderate or greater turbulence in practice, this problem should not have significantly affected the skill of the test forecast method.

Threshold determination also provided several noteworthy results not listed in Table 6. First, there were only 24 instances of severe turbulence in this sample making

determination of the thresholds for that intensity unreliable. This led to the establishment of an almost arbitrary value for the severe turbulence thresholds and no value being determined for the MWFM V1.1 index severe threshold. As such, any indication of severe turbulence by the forecast method was ignored for this study and only moderate regions were highlighted for the verification study of Section 4.3. Additionally, the χ^2 test was performed on the contingency table produced by the combined thresholds for moderate turbulence. The resulting value of 193.5323 suggested there was a $5.39 \times 10^{-42}\%$ chance of incorrectly rejecting the null hypothesis with this χ^2 value. This provided strong evidence to reject the null hypothesis and conclude the index values offer some skill in predicting turbulence. Another interesting fact of this test was that FAR did not increase with the addition of MWFM indices to the forecast. In fact FAR decreased from 0.8394 to 0.8339 to 0.8338 as the MWFM indices were added to Ellrod-2 index when computing the moderate layer threshold. This provides another indication that the MWFM indices improve the forecast. Additionally, the MWFM indices provide a larger improvement in the PODy than the degradation in the PODn, suggesting they add value to the forecast.

After determining the thresholds, it was necessary to see if they change significantly for different geographic regions or altitudes. This test was performed by setting the indices to the established thresholds and calculating the statistics over different regions or altitudes. For this test, there were nine different regions tested for moderate turbulence. The regions included the following areas: A) Entire region, B) FL100-FL200, C) FL200-FL300, D) FL300-FL400, E) FL400-FL500, F) 110W-70W and 20N-40N, G) 110W-70W and 40N-60N, H) 70W-30W and 20N-40N, and I) 70W-30W and

40N-60N. The resulting statistics are listed in Table 7. The statistics varied considerably for different regions and levels in the atmosphere suggesting different thresholds based on geographic region or altitude might produce more accurate results. In addition, several of these samples failed the χ^2 test for independence. Those tests include E, H, and I with χ^2 values of 2.00, 1.38, and 3.44 respectively. Each of these χ^2 values, with an α of 0.05, fail to reject the null hypothesis. In test H, the “yes/yes” cell only expected 1.62 occurrences. According to Wilks (1995), cells containing less than five instances of an expected event should be avoided. Also, in tests H and I, there were only 13 and 35 positive reports of moderate or greater turbulence. This lack of positive reports decreased the credibility of the statistics listed for those rows. Despite the lack of validity regarding these two regions, there does appear to be some regional variation in the thresholds.

Table 7. Statistics for different regions

Test	Sample Size	PODy	PODn	FAR	CSI	PC	BIAS	TSS	HSS	GSS
A	15745	0.5628	0.5983	0.8225	0.1560	0.5935	3.1703	0.1611	0.0840	0.0438
B	2136	0.5367	0.6001	0.6004	0.2971	0.5791	1.3432	0.1369	0.1260	0.0672
C	1161	0.6187	0.5102	0.6240	0.3053	0.5452	1.6453	0.1288	0.1102	0.0583
D	11987	0.5696	0.6030	0.8911	0.1006	0.6004	5.2295	0.1726	0.0588	0.0303
E	463	0.4487	0.6364	0.8000	0.1606	0.6048	2.2436	0.0851	0.0569	0.0293
F	4837	0.5555	0.6466	0.6498	0.2735	0.6233	1.5862	0.2021	0.1694	0.0925
G	4922	0.5822	0.5503	0.7913	0.1815	0.5557	2.7899	0.1325	0.0774	0.0402
H	869	0.2308	0.8773	0.9722	0.0254	0.8677	8.3077	0.1081	0.0235	0.0119
I	5167	0.6000	0.5563	0.9909	0.0091	0.5566	65.6571	0.1563	0.0047	0.0024

4.3 Forecast Comparison

To compare forecast skill, 12-hour and 24-hour forecasts were made using the test method and verified with PIREPS. Additionally, 12-hour and 24-hour operational forecasts produced by the Air Force were also verified with PIREPS. When initially

attempting to implement the test method as an operational forecast tool, the indices produced output that was very confusing and that would have been difficult to use operationally. The composite images produced with these thresholds were very congested with contours, as depicted by the image on the left in Figure 7. As a result, the composite image only depicted regions with turbulence when three adjacent layers indicated turbulence at a grid point as described in section 3.4.3. This modification produced the image on the right in Figure 7 which was much easier to contour.

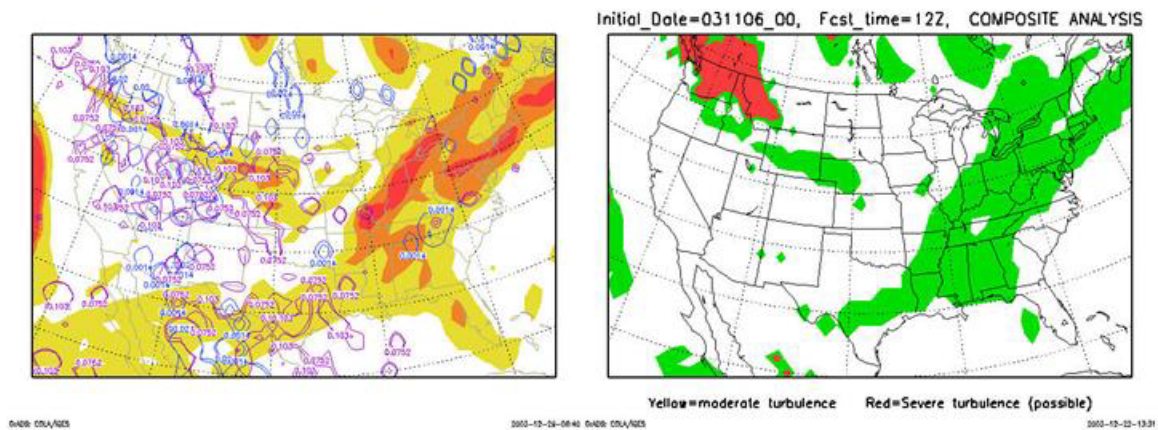


Figure 7. Examples of composite level output

After adjusting the method for computing the composite chart, forecasts were made using the test method. Typically, these hand-plotted forecasts took less than five minutes to produce. Next, these test forecasts and actual forecasts produced by operational weather squadrons were verified for accuracy with PIREPS from October 21, 2003 to October 27, 2003 and from November 5, 2003 to November 12, 2003. To verify, PIREPS were compared by location and height to the forecasts. In order to be counted, PIREPS needed to be above the CONUS since the weather squadrons did not forecast

outside the CONUS. When a PIREP fell within a region highlighted to suggest turbulence, it was considered forecasted. Only PIREPS of moderate or greater intensity were considered observed.

The PIREPS were plotted using GrADS on a chart that contained the test method forecast regions so the comparison was quite accurate for the test method. Operational forecasts were compared with PIREPS using estimation. To ensure the weather squadron forecast skill was maximized, PIREPS appearing very close to a region of forecasted turbulence were given the benefit of the doubt. In general, these events were scored as either “yes/yes” or “no/no”. Furthermore, this study only predicted regions of moderate or greater turbulence. There were many PIREPS of light turbulence reported in forecasted regions of moderate turbulence. Those regions were scored as forecasted “yes” but observed “no” or “yes/no”. The test method and operational forecast contingency tables are provided in tables 8 and 9. The χ^2 test scores of 189.9 for the test method and 35.97 for the operational forecasts are sufficient to reject the null hypothesis leading to the conclusion that forecasts and observations are not independent.

Table 8. Test method contingency table

		Observed	
		Yes	No
Forecasted	Yes	325	478
	No	246	1371

Table 9. OWS forecast contingency table

		Observed	
		Yes	No
Forecasted	Yes	87	130
	No	484	1719

These tables suggest significant differences exist in the two methods. In general, the operational forecasts tend to significantly under forecast turbulence event relative to the test method, as evidenced by the large number in the “no/yes” cell. At the same time, the test method appears to significantly over forecast turbulence. This apparent weakness is tempered by the short-lived nature of CAT and the low reliability of the “yes/no” cell as a determinant of forecast skill. Also, negative reports of turbulence would often appear very close to positive reports of turbulence in time and location further validating the claim that CAT is short-lived and localized. Also, the operational forecasts did not appear to consider turbulence caused by mountain waves. There was not one region depicted on the charts over these two weeks where the weather squadrons used solid blue lines to depict mountain wave turbulence. This may be due to mislabeling since there were several regions which suggested the forecaster considered the turbulence to be mountain wave turbulence although they used the general CAT line style to circle them.

Table 10. Verification statistics

	PODy	PODn	FAR	CSI	PC	BIAS	TSS	HSS	GSS
Test Method	0.569	0.741	0.595	0.310	0.701	1.406	0.311	0.272	0.231
Operational Forecasts	0.152	0.930	0.599	0.124	0.746	0.380	0.082	0.104	0.114

Instances where the test method did not forecast regions that observed turbulence were explored further to determine the cause. There were several possible reasons the test method did not highlight these regions of turbulence. Several observed instances of turbulence appear to have been caused by convection. These instances would not meet the definition of CAT but were left in the tables since this is a comparative study of

forecast methods and, in general, neither method forecasted those regions. The most common cause of missed regions of turbulence was near misses where the turbulence appeared just outside of the highlighted areas. Many of these near misses were captured with the actual layer viewer. Table 10 provides the detailed breakdown of the statistics produced from the contingency tables for the test method and operational forecasts.

The test method appears superior to operational forecasts. The test method scored significantly higher POD_y, TSS, HSS, and GSS over the operational forecasts. The higher POD_n of the operational forecasts is due in large part to the significantly lower volume coverage of the forecasts. The bias scores suggest the test method tends to over-forecast turbulence while the operational forecast tends to under-forecast turbulence. However, the test method bias is closer to one suggesting it tends to over-forecast less than the operational forecast tends to under-forecast.

V. Conclusions and Recommendations

5.1 Conclusions

For many years, meteorologists have attempted to predict occurrences of clear-air turbulence. In recent years, various numerical indices have been developed and tested to quantitatively predict CAT. It had been shown that numerical models outperform conceptual models when forecasting CAT (Dutton 1980). This study seems to back up that assertion. This research focused on developing a new technique for predicting CAT that incorporated three numerical model indices, the Ellrod-2 index and the two MWFM indices. Including tools for predicting both primary causes of CAT provided a comprehensive prediction method. The technique was developed to meet the needs of Air Force operational weather squadron forecasters for a comprehensive, easy-to-use automated forecast method. Furthermore, the technique is adaptable to indices other than those chosen in this study.

The mountain wave forecast model indices showed promise in predicting CAT regions in the troposphere. The V2.1 index provides more comprehensive coverage than the V1.1 index. However, MWFM V2.1 does not appear to capture every region of mountain wave turbulence, and the V1.1 index appears to add some value to the overall forecast. Although most turbulence encounters appear to be represented by an index depicting Kelvin-Helmholtz instabilities, there were several instances that the MWFM captured but that the Ellrod-2 index missed. In this study, the mountain wave indices

appeared to capture about one in every ten correctly forecasted moderate or greater turbulence encounters throughout the column, not just near the tropopause.

The test method appears to provide superior forecasts to those currently produced by the operational weather squadrons who appear to primarily use conceptual models in their turbulence chart development. This is most likely the cause of the significant under-forecasting and inaccuracy in the weather squadron products used for this research.

While the test method provided a large number of near misses on occurrences of turbulence, PIREPS of turbulence were often quite far from the nearest turbulent region indicated by the weather squadron forecasts. However, the test method charts tend to encompass a large portion of the atmosphere making turbulent conditions appear quite widespread. Furthermore, the test method appears to miss quite a few instances of turbulence despite the layer viewer depicting those regions as turbulent. These misses are caused by the implementation of the composite chart as described in Section 3.4.3. Also, because of the significant coverage of turbulent regions by the test method, using the test method is not as straightforward as initially thought. This was especially true over the Rocky Mountains as they often have numerous levels and layers where the mountain wave forecast models predicted turbulence.

This study only focused on moderate or greater turbulence. The length of time used in this study did not provide an adequate number of severe PIREPS (due to their limited availability) to properly threshold severe turbulence events. The few instances of severe turbulence actually depicted in this study did allow for some degree of threshold determination; however, the results are unreliable and, therefore, deemed inconclusive. Properly thresholding severe turbulence would require a much longer test period,

encompassing many more severe turbulence encounters than identified in the sample analysis.

Overall, the test method appears to offer promise as a tool that simplifies an otherwise complex process. The time required to develop forecasts for the CONUS using this new tool should be less than five minutes per forecast hour shortly after the forecaster masters the technique and the OPS II drawing features. Furthermore, the largely objective nature of the method will reduce the inconsistency between forecasters and lessen the impact of inexperience on the reliability of the product.

Although this method was developed for turbulence, similar techniques using a composite chart and layer viewer may provide additional benefits in other areas of forecasting such as for aircraft icing. Additionally, the layer viewer can be used to aid the forecaster in synoptic scale analysis and forecasting.

5.2 Recommendations

5.2.1 Recommendations to AFWA and 15th OWS. This method appears to offer a superior, comprehensive tool in developing upper level turbulence charts. It allows a large portion of the globe to be quickly analyzed for turbulence. Furthermore, a method very similar to the test method has been used operationally at the 17th OWS for over two years. The OPS II script employed by the 17th OWS generates a composite chart and layer viewer charts very similar to those developed for this study. However, the script used at the 17th OWS does not include mountain wave turbulence and only used output from two adjacent layers instead of the three layers used in this study.

It is strongly recommended AFWA run the mountain wave forecast model V1.1 and V2.1 for the troposphere and converts that output into a format suitable for use by OPS II. If it is necessary to make the data match gridded output, it is suggested AFWA use the same approach employed in this study. Furthermore, the layer viewer html and javascript code should be provided to the operational weather squadrons for their immediate implementation. The code developed for this method can be easily modified by the weather squadron web masters and used to supplement or replace current techniques.

Finally, to better meet the needs of aircrews, it is recommended that weather packages include the traditional turbulence chart, as generated by the test method, along with several layer-specific charts based on unanalyzed model output near the flight level of the aircraft. This provides the pilot with a general idea of the turbulent regions, as well as, the areas of potential turbulence at the levels they are flying. Providing both charts will offer the most complete picture of where the aircrew might experience turbulence and what their best course of action might be to avoid the turbulence if necessary.

5.2.2 Future Research Recommendations. There are numerous additional research studies that may be performed to further test the methods developed here. The test performed in Table 7 suggests the indices' thresholds may vary based on levels of the atmosphere and geographical locations of the aircraft. Additional studies to determine if the thresholds vary based on those criteria might be performed. Furthermore, this study used GFS model data to determine the Ellrod-2 index and initialize the mountain wave

forecast model. Using higher resolution model data might provide more accurate results than using the data chosen here.

This study focused on determining regions of moderate turbulence using data over a five month period to calibrate the indices. Additionally, the study only verified forecasts for two weeks in the fall. This limited study was adequate to demonstrate the relative skill of the test method to operational forecasts but further studies using a larger dataset might allow accurate calibration of severe turbulence thresholds and it might provide insight into how the index thresholds change with different seasons. Future studies might also use PIREPS that include aircraft type to more accurately assess intensity reports. Also, no steps were taken to initialize or verify the GFS model using to compute the indices before making the forecasts. Taking those steps might further increase the accuracy of the forecast method.

This study only tested three indices in predicting CAT, using the Ellrod-2 turbulence index as a means of determining CAT caused by Kelvin-Helmholtz instabilities. There are many other indices developed to predict CAT caused by Kelvin-Helmholtz instabilities. Future studies might consider using a different index or using an ensemble forecast of sorts with several different indices to determine if they provide more accurate results. These ensembles might rely on several indices on a layer indicating turbulence as opposed to this study's reliance on several different layers depicting turbulence to mark an area with turbulence. Additionally, future versions of the MWFM or other mountain wave models might become available that would require testing to determine their use.

Finally, this method is a step towards completely automating the CAT product produced by weather squadrons. It seems a similar method using sets of rules could be developed to produce a chart without any forecaster involvement at all. This method might reduce the forecaster's role to quality control checking the chart and adjusting regions based on model error in initialization or verification purposes only. This would further simplify the CAT forecast process and essentially eliminate the forecaster from being in the loop for CAT prediction altogether.

Appendix A: Detailed Computations

1. Computations involved in MWFM V1.1 (Bacmeister et al. 1993). This is designed to provide a basic understanding of the underlying equations involved in computing turbulence with the Mountain Wave Forecast Model.

First, the local saturation limit is computed

$$\delta_{sat,k}(z) = \frac{U_{\perp;k}(z)}{N_k(z)}$$

Then, a first guess of the wave displacement profile at a level is made using

$$\delta_k^*(z + \Delta z) = \delta_k(z) \left[\frac{\rho(z)N_k(z)U_{\perp;k}(z)}{\rho(z + \Delta z)N_k(z + \Delta z)U_{\perp;k}(z + \Delta z)} \right]^{1/2}$$

If this value is more than the saturation limit, it is reduced to the saturation limit. To compute the value at the surface, use the minimum of saturation value at the surface and $4a_k$ where a_k is a ridge height parameter. Now, the momentum flux is approximated by

$$\phi_k(z) \approx \alpha \rho(z)N_k(z)U_{\perp;k}(z) \frac{\delta_k(z)^2}{L}$$

and this is used to compute turbulence by

$$KE_{Turbulence} \left(z + \frac{\Delta z}{2} \right) \propto \phi_k(z) - \phi_k(z + \Delta z)$$

The definition of the terms:

$\delta_{sat,k}$	local saturation limit of wave-induced vertical displacement
$U_{\perp;k}$	perpendicular wind component to the ridge based on height
N_k	Brünt-Väisala frequency
δ_k^*	first guess of wave-induced vertical displacement at a level
ρ	density of the air at a level
α	dimensionless ridge-shape factor
L	horizontal length representing extent of wave disturbance
ϕ_k	average momentum flux at level k
$KE_{Turbulence}$	The turbulence produced by waves from lost momentum flux

2. Haversine method used to calculate distances on this sphere. Method as presented in Sinnott (1984) used extensively to calculate distances. Function passes two sets of latitude and longitudes and returns the distance between them.

$$d_{lat} = lat_2 - lat_1 \quad d_{lon} = lon_2 - lon_1$$

$$a = \sin\left(\frac{d_{lat}}{2}\right)^2 + \cos(lat_1) \cos(lat_2) \sin\left(\frac{d_{lon}}{2}\right)^2$$

$$c = 2 \arctan\left(\frac{\sqrt{a}}{\sqrt{1-a}}\right)$$

$$dist = earth_radius \times c$$

Appendix B: CONUS what2do Script

This is the what2do script used by this research to run the MWFM V1.1 and V2.1. The what2do files are located in the /MWFM/source/jobs/what2do/ directory. Its primary function is to set up the variables which control how the experiment runs. To run a new experiment, one must modify several other scripts including:

1. /MWFM/source/jobs/what2do/special_cases.pro: set up a new special case with this number by copying and pasting another special case and modifying it as needed.
2. /MWFM/source/jobs/progs/at_glider.pro: add new special case.
3. /MWFM/source/jobs/drivers/drv_glider.pro: add new special case.
4. /MWFM/source/core/frst_mtnwave.pro: add new special case.

```
PRO WHAT2DO_BELSONTEST,date=date,pole=pole,xrang=xrang      $
  ,field=field,levels=levels,latlonlims=latlonlims           $
  ,what=what,source=source,grid=grid                          $
    ,sequence=sequence,special=special                       $
    ,psfile=psfile,mwfmversion=mwfmversion                   $
    ,srcplane=srcplane,strict18=strict18,map_ann=map_ann     $
    ,plot_items=plot_items
```

```
;+
;
;
;=====
; |   (   )   (   |
; | M ) W ( F ) M |
; |   (   )   (   |
; | _____/^\_____/\^_____/\^_____ |
; | Mountain Wave Forecast Model |
; |_____~
;-----
; WHAT2DO_BELSONTEST
;-----
; template what2do_XXXX.pro routine to set up a new MWFM experiment: replace
; "XXXX" with your experiment name and change various what.* values below to
; tune to your specific experiment, then set up your own drv_XXXX.pro
; (MWFM 1.*) or specialcase in special_cases.pro (MWFM 2.*).
;
```

```

;-----
; MWFM USAGE      e.g., special_cases.pro (source/jobs/what2do)
;   LOCATION      source/jobs/what2do
;
;-----
; HISTORY
; 20020811 SDE: created as a standardized what2do template from cleaned,
;               commented, and documented what2do_usarrayforecast.pro
;
;-----
; KEYWORDS/PARAMETERS
;
; date            input of standard character date in YYYYMMDD or YYYYMMDDZZ
;                 format: gets plugged into what.date. You should always
;                 pass a date, otherwise you'll get an unsatisfactory
;                 default
; pole            2-element vector of the "map pole" or center of the map,
;                 in the format [longitude,latitude]. If not input, uses a
;                 default value set below: gets plugged into what.pole
; xrang           2-element x range vector for GSFC map sizing, used
;                 explicitly only for map_source=0. For new IDL maps it
;                 is only used unless the (much preferred) explicit sizing
;                 option "platonlims" in the pltrec structure (i.e.,
;                 pltrec.platonlims) is not set. If not input, uses a
;                 default value set below: gets plugged into what.xrang
; field           multi-element vector (# elements corresponding to the
;                 number of requested forecast plots), containing integer
;                 MWFM wave field indicies corresponding to various MWFM
;                 output fields that can be calculated. Type
;                 FIELD_STRINGS, /LIST within MWFM to see currently
;                 supported list of permitted wave field indices and what
;                 they correspond to. If not input, field is set to
;                 default values set below: field gets plugged into
;                 what.field
; levels          a multi-element vector of exactly the same size as field
;                 that represents the integer index values of the pressure
;                 at which you wish to do this forecast. This is dependent
;                 on the pressure level array of your particular atmospheric
;                 data source: MWFM has pressures that go from largest
;                 (low altitude) to smallest (highest altitude), so that if
;                 the pressure level array is [1000.0,925.0,850.0,700.0....]
;                 then level=[0,1,3] tells MWFM to plot 3 forecasts: first
;                 on the 1000hPa surface, second on the 925hPa surface and
;                 the third on the 700hPa surface. The field plotted in
;                 each case is given by the field array above: e.g.,

```

```

;         field=[0,0,0] will plot peak vertical displacements in
;         each case. To find out allowable pressure surfaces, you
;         will need to read your data in using get_glbdata.pro and
;         then print out the returned plev array. If not input,
;         levels is set to default values set below: levels gets
;         plugged into what.levels
; latlonlims    a 4-element array that defines the regional
;               longitude-latitude bounds [lonmin,lonmax,latmin,latmax]
;               within which MWFM will do the forecast. For example,
;               latlonlims=[-10.0,30.0,60.0,70.0] performs a forecast
;               in the longitude range 10W to 30E and for latitudes
;               between 60N and 70N, which corresponds roughly to
;               Scandinavia. See get_glbdata.pro for more
;               information/context. If not input, latlonlims is set to
;               default values set below: latlonlims gets plugged into
;               what.latlonlims
; what         the output "what2do" structure that this routine returns,
;               containing all the information and switches needed to
;               run this particular MWFM forecast/analysis run just the
;               way the user wants. See the structure assignment
;               statement below for all the information within it and
;               what it all means, or else type HELP, what, /STRUCTURES
;               after calling this routine using what=what
; source       specify the source string: type GET_GLBDATA,/LIST to get
;               listing of currently supported atmospheric data sources.
;               e.g., source='NMC' specifies NCEP/NMC data. If not input,
;               source is set to default values set below: source gets
;               plugged into what.source
; grid        the grid string in GSFC format: e.g., 'GG2%5X2%5' for 2.5x
;               2.5 degree lon-lat gridding in the file. Gets plugged into
;               what.grid
; sequence    the sequence data string in GSFC format, e.g., 'E01'
; special     the special data string in GSFC format, again identifying
;               the specific kind of atmospheric data file we're reading
; psfile      if set true, activates postscript output via what.psfile=1
; mwfmversion passes the MWFM version (1, 2, ....)
; srcplane    string used to signify the source of aircraft data to be
;               overplotted (e.g., 'ER2')
; strict18    older keyword in which atmospheric data at 18 standard
;               pressure levels is strictly enforced. If press=-1
;               then it requires data at all X levels (I think)
; map_ann     older map annotation keyword
; plot_items  another plot annotation device, this time a structure
;               used to annotate something to a plot. For a sample, see
;               code in what2do_solve.pro

```

```

;
;
;
;*****
;AUTHORIZATION TO USE AND DISTRIBUTE
;*****
;I hereby agree to the following terms governing the use and redistribution of
;The NRL Mountain Wave Forecast Model (MWFM), mountain wave forecasting
;and display software, written and developed by Stephen D. Eckermann and
;colleagues at Code 7646 at the Naval Research Laboratory in Washington, DC.
;
;Redistribution and use in source and binary forms, with or without
;modification, are permitted provided that: (1) source code distributions
;retain this paragraph in its entirety, (2) distributions including binary
;code include this paragraph in its entirety in the documentation or other
;materials provided with the distribution, and (3) all advertising materials
;mentioning features or use of this software display the following
;acknowledgment: "This product includes software written
;and developed by Stephen D. Eckermann and colleagues of the Naval
;Research Laboratory (NRL)." Neither the name of NRL or its contributors, nor
;any entity of the United States Government may be used to endorse or promote
;products derived from this software, nor does the inclusion of the NRL written
;and developed software directly or indirectly suggest NRL's or the United
;States Government's endorsement of this product.
;
;THIS SOFTWARE IS PROVIDED "AS IS" AND WITHOUT ANY EXPRESS OR
IMPLIED
;WARRANTIES, INCLUDING, WITHOUT LIMITATION, THE IMPLIED
WARRANTIES OF
;MERCHANTABILITY AND FITNESS FOR A PARTICULAR PURPOSE.
;*****
;*****
;
PRINT, '*****'
PRINT, '***** what2do_belsontest *****'
PRINT, '*****'
PRINT, '*****'

IF (NOT KEYWORD_SET(mwfmversion)) THEN mwfmversion=1 ;default to old
MWFM 1.*
;
; we must have a date
;
IF (NOT KEYWORD_SET(date)) THEN BEGIN
date='00012300'

```

```

DATE2STRING, date, sdate=sdate, /cen, hour=hour
MESSAGE, '      *****WARNING*****      ',/INFORMATIONAL
MESSAGE, 'Date string not input as keyword date=date', /INFORMATIONAL
MESSAGE, 'Choosing default of '+sdate+', '+hour+'Z', /INFORMATIONAL
MESSAGE, '      *****END WARNING*****
',/INFORMATIONAL
ENDIF
;
; set the atmospheric data source as defined in the GSFC-like method by 4
; character strings: source=major source of the data, sequence=basic type
; of forecast/analysis from this source, special is a special identifier
; associated with sequence variations, and grid is the latitude-longitude
; resolution of the atmospheric gridding (e.g., grid='GG2%5X2' means 2.5
; degrees longitude by 2 degrees latitude)
;
IF (NOT KEYWORD_SET(source)) THEN source='NMC' ELSE $
  source=STRCOMPRESS(STRUPCASE(source),/REMOVE_ALL)
IF (NOT KEYWORD_SET(grid)) THEN grid='GG1X1'
IF (NOT KEYWORD_SET(sequence)) THEN sequence='pre'
IF (NOT KEYWORD_SET(special)) THEN special=""

;
; check/set up field and level arrays for all the necessary plots
; see FIELD_STRINGS, /LIST for permitted fields and their field code
; see plevs from get_glbdata.pro for range of permitted level indices
;

IF NOT KEYWORD_SET(field) THEN BEGIN
  CASE source OF
    'ASM': field=[0,2,0,2,0,2]
    ELSE: field=[2,2,2,2,2,2,2,2,2,2,2,2,2,2,2,2] ; Output 16 turbulence charts
  ENDCASE
ENDIF

; set pressure levels to output
;
; 10=70mb
;
; 11=50mb 12=30mb 13=10mb 14=5mb 15=2mb 16=1mb, 17=0.4mb
;

IF NOT KEYWORD_SET(levels) THEN BEGIN
  CASE source OF
    'ASM': levels=[10,10,16,16,19,19]
    ELSE: levels=[5,6,7,8,9,10,11,12,13,14,15,16,17,18,19,20] ; Output levels 850-100
mb
  ENDCASE
; array same length as field

```

```

ENDIF

;
; check field and level array lengths, then set number of plots (nplots)
;

IF (N_ELEMENTS(field) NE N_ELEMENTS(levels)) THEN BEGIN
  MESSAGE, '          *****WARNING*****          '/INFORMATIONAL
  MESSAGE, 'field & levels do not have the same # elements', $
  /INFORMATIONAL
  MESSAGE, $
  'longer array will be truncated to make sizes the same', $
  /INFORMATIONAL
  MESSAGE, '          *****END WARNING*****          '
'/INFORMATIONAL
  nplots=MIN([N_ELEMENTS(field),N_ELEMENTS(levels)])
ENDIF ELSE $
  nplots=N_ELEMENTS(field)

MESSAGE, STRTRIM(STRING(nplots),2)+' MWFM Plots have been requested', $
  /INFORMATIONAL

IF NOT KEYWORD_SET(latlonlims) THEN BEGIN
  latlonlims=[-140.,-30.,20.,60.] ;set for CONUS
ENDIF ELSE $ ;100 150

  IF N_ELEMENTS(latlonlims NE 4) THEN BEGIN
    PRINT, 'latlonlims = ',latlonlims
    MESSAGE, ' latlonlims must be a 4-element vector'
    RETURN
  ENDIF

;
; set map sizes and center/"pole" location
;

IF NOT KEYWORD_SET(xrang) THEN BEGIN ;pltrec.latlonlims can also be used
  xrang=[-0.425,0.425] ;set your own preferred default xrang here
  xrang=[-0.25,0.25]
ENDIF

IF NOT KEYWORD_SET(pole) THEN BEGIN
  pole1=[-130.0,39.]
; pole2=[-100.0,39.] ;set your own preferred map poles - the pole1
  pole2=pole1 ;& pole2 arrays allow the user to choose alternating

```

```

;map zones, originally created for east coast and
;west coast US zooms for USA MWFM forecasts
ENDIF

;
; mirror these values into pole, x range and data range values for each plot
; in the range 1...nplots
;

poles = FLTARR(2,nplots)
xrangs = FLTARR(2,nplots)
drangs = FLTARR(2,nplots)

;
; nominal data ranges for various MWFM fields: see FIELD_STRINGS, /LIST for
; details on the physical quantities and units
;

drang0 = [ [0.,1000.] $ ;peak vertical displacement amplitudes (m)
, [0.,10. ] $ ;Eliassen Palm Fluxes (Pa)
, [0.,3.0] $ ;turbulence intensities (J/m^3)
, [0.,20.] $ ;peak temperature amplitude (K)
, [0.,20.] $ ;peak total horizontal vel. amp. (m/s)
, [0.,2. ] ] ;peak vertical velocity amplitude (m/s)

;
; store poles and ranges for each plot
;

FOR i = 0,nplots/2-1 DO BEGIN
  poles(0,i*2) = pole1
  poles(0,(i*2+1)) = pole2
ENDFOR
FOR I = 0,NPLOTS-1 DO BEGIN
  xrangs(0,i) = xrang
  drangs(0,i) = drang0(*, field(i) )
ENDFOR
;
; other plot/data-related default setups....
;
IF NOT KEYWORD_SET(psfile) THEN psfile=1
IF NOT KEYWORD_SET(srcplane) THEN srcplane=""
IF NOT KEYWORD_SET(strict18) then strict18=0
IF NOT KEYWORD_SET(map_ann) THEN map_ann=0
IF NOT KEYWORD_SET(plot_items) THEN plot_items=0

```

```

=====
;
;-----
; create the "what" (what2do) structure
;-----
=====

what={
    date:date,          $          ;date string
    source:source,     $          ;atmospheric source string
    grid:grid,         $          ;grid string
    sequence:sequence, $          ;sequence identifier for source
    special:special,   $          ;special identifier for source
    GRIB:1,            $          ;use GRIB format
;   press:[1000.00,925.000,850.000,700.000, $
;   500.000,400.000,300.000,250.000,200.000,150.000,100.000,70.0000, $
;   50.0000,30.0000,20.0000,10.0000] , $
;   press:-1 ,        $ ;set to -1 for non-18 levels (e.g., TRMM)
;
;                       ;comment out for 18 standard pressures
;
;                       ;set to whatever for GRIB picking of levs
    nazimuths:18,     $          ;# azimuths in ray forecasts
    nkvals:2,         $          ;# horiz. wavenumbers if rayfcst
;   filter:0,         $          ;filter MWFm data?
;   minlz:5.0,        $          ;min. vert wavlgth to filter (km)
;   minlh:100.0,      $          ;min. horz wavlgth to filter (km)
;   amp_crit:200.0,   $          ;crit. vdisp for mak_rayini
    latlonlims:latlonlims, $      ;latlonlims array
    only:4,           $          ;orig_wd tag for ridge database
;   units:",          $          ;unit string
;   label:",          $          ;label string
    forecast:'0',     $          ;forecast flag
    zerohourforecast:1 , $        ;for fh=0 assumes fcst not anal
    nplots:nplots,   $          ;number of plots to do
;   interact:0,       $          ;interactively get vals
    autoscale:1 ,    $          ;automatic color bar scale?
    densscal:1 ,     $          ;1 -> dens-scaled momflux
    colortable:0 ,   $          ;color table to use
    metparam:'z' ,   $          ;overplot what form of data?
;   metlevels:findgen(30)*2+180. , $ ;use these contour levels
    met_charsize:0.2 , $         ;charsize contour met labels
;   snatplot:0 ,     $          ;plot NAT supersaturation
;   nometdata:0 ,    $          ;no met data on plot
    boxes:1,         $          ;plot ridges as ridge boxes
;   vectors:0 ,      $          ;plot wind vectors?
    field:field ,    $          ;field indices to plot

```



```

levels:levels ,      $      ;level indices @which to plot
strict18:strict18 ,  $      ;strict 18 flag
; batch:0,           $      ;older batch mode
; traj:0,            $      ;older trajectory dump option
datadump:1,          $      ;dump data offline or not
powerav:1,           $      ;power index 4 offline average
xavint:0.5,          $      ;averaging interval (longitude)
yavint:0.5,          $      ;averaging interval (latitude)
poles:poles,         $      ;map poles
drangs:drangs,       $      ;data ranges (for autoscale=0)
xrangs:xrangs,       $      ;x map ranges
giffile:0,           $      ;export a GIF file?
; gifname:date+'.gif', $      ;specify gif file name
psfile:psfile,       $      ;export a PS (postscript) file?
pstag:'temp'+date,   $      ;character filename for psfile
colorps:1,           $      ;color postscript?
; noreverse_pscols:1, $      ;forces nonreversal of color
towebsite:0,         $      ;transfer plots to web?
; webscript:'ToWebSite_Glider', $ ;web transfer script to use
hardcopy:0,          $      ;print out a hard copy
; noflt_trk:1,       $      ;do/don't plot flight track
srcplane:srcplane }

```

```

RETURN
END

```

Appendix C: GrADS Scripts

There were three files necessary to use GrADS for this research. The first defines the metadata file. It is called either test12.ctl or test24.ctl. The second uses the GrADS scripting language to build the different layers used in the layer viewer. The third file uses the GrADS scripting language to verify the forecasts by plotting PIREPS on the chart.

```
1.
DSET ^out12.dat
UNDEF 9999
TITLE Knapp Ellrod and Mountain Wave Indices
*
XDEF 111 LINEAR -140.0 1.0
*
YDEF 41 LINEAR 20.0 1
*
ZDEF 14 LINEAR 100 50
*
TDEF 1 LINEAR 06NOV2003 1DY
*
VARS 4
h 14 99 average height of layer
ke 14 99 Knapp Ellrod Index
mw1 14 99 Mountain Wave V1
mw2 14 99 Mountain Wave V2
ENDVARS
```

```
2.
* This program builds the desired files the way I want it to
prompt 'Enter the desired date: '
pull date1
hr='00'
time=12
date2=date1'_'hr
'set annot 0'
'set background 1'
'set xlopts 0'
'set ylopts 0'
'set line 0'
```

```

'set grid on 5 0'
'c'
while (time <= 24)
  level=700
  llevel=750
  'open 'date2'/test'time'.ctl'
  say '*** Opened 'date2' test'time'.ctl for analysis ***'
  while (level >= 100)
    'set mproj nps'
    'set mpvals -120.5 -75.5 25 52'
    'c'
    'set lev 'level'
    'set map 0 1 1'
    'set mpdset mres'
    'set gxout shaded'
    'set clevs 3 6 8.37'
    'set ccols 1 7 8 2'
    'd ke'
    'set gxout contour'
    'set clab off'
    'set clevs 0.0014 99.0'
    'set ccolor 4'
    'd mw1'
    'set clab off'
    'set clevs 0.0752 0.103'
    'set ccolor 9'
    'd mw2'
    'draw title Initial_Date='date2', Fcst_time='time'Z, Layer='level'-'llevel'mb'
    'draw xlab Shaded=Ellrod-2 Blue=MWFM V1.1 Purple=MWFM V2.1'
    'wi 'date2'/'time'_level'level'.jpg'
    level=level-50
    llevel=llevel-50
  endwhile
  'c'
  'set lev 750'
  'set gxout shaded'
  'set clevs 1 2'
  'set clab off'
  'set ccols 1 3 2'
  'd h'
  'draw title Initial_Date='date2', Fcst_time='time'Z, COMPOSITE ANALYSIS'
  'draw xlab Yellow=moderate turbulence Red=Severe turbulence (possible)'
  'wi 'date2'/'time'_all.jpg'
  'c'
'close 1'

```

```
time=time+12
endwhile
```

3.

* This program builds the desired files the way I want it to

* Variables to decipher PIREP location

```
say 'Hello. PIREP display program.'
```

```
x_len=10
```

```
y_len=7
```

```
x_int=x_len/(140-30)
```

```
y_int=y_len/(60-20)
```

```
date1=1
```

```
hr='00'
```

* Sets up the basics of the map

```
'set xsize 880 680'
```

```
'set mproj scaled'
```

```
'set annot 0'
```

```
'set background 1'
```

```
'set xlopts 0'
```

```
'set ylopts 0'
```

```
'set line 0'
```

```
'set grid on 5 0'
```

```
'set background 1'
```

```
'set rgb 16 225 225 225'
```

```
'set rgb 17 200 200 200'
```

```
'set rgb 18 175 175 175'
```

```
'c'
```

```
level=750
```

* Loops until the quit option is chosen

```
while ((date1 != 0) & (date1 != ""))
```

```
  say '*****'
```

```
  say 'PIREP Verification'
```

```
  say '*****'
```

```
  prompt 'Enter the desired date (0 signifies quit): '
```

```
    pull date1
```

```
  date2=date1_'hr'
```

```
  if ((date1 != 0) & (date1 != ""))
```

```
    tme=12
```

```
    while (tme <= 24)
```

```
      'set mproj scaled'
```

```
      'set annot 0'
```

```
      'set background 1'
```

```
      'set xlopts 0'
```

```
      'set ylopts 0'
```

```

'set line 0'
'set grid on 5 0'
'c'
date3=date2'/test'tme'.ctl'
'open 'date3
say ' Opened 'date2' test'tme'.ctl'
'c'
'draw title Date 'date2' file=test'tme'.ctl'
'set lev 'level
'set map 15 1 1'
'set mpdset mres'
'set clevs 1 2'
'set ccols 17 18'
'set gxout shaded'
'd h'
r1ec=0
c1=1
while (r1ec != 2)
  date4=date2'/out'tme'.txt'
  r1=read(date4)
  r1ec=substr(r1,1,1)
  if (r1ec != 2)
    lat=substr(r1,3,5)
    if (substr(r1,15,1) = '  ')
      lon=substr(r1,9,6)
      hour=substr(r1,27,2)
      hgt=substr(r1,30,5)
      ti=substr(r1,36,1)
    else
      lon=substr(r1,9,7)
      hour=substr(r1,28,2)
      hgt=substr(r1,31,5)
      ti=substr(r1,37,1)
    endif
    if ((lat >= 25) & (lat <= 50) & (lon >=-130) & (lon<=-60))
      x=(140+lon)*x_int+0.5
      y=(lat-20)*y_int+0.75
      if (ti = 0)
        ti2=0
        ms=1
      endif
      if (ti = 1)
        ti2=3
        ms=3
      endif
    endif
  endif
endwhile

```

```

if (ti >= 2 & ti <= 5)
    ti2=7
    ms=5
endif
if (ti >= 6)
    ti2=2
    ms=9
endif
'set line 'ti2
'draw mark 'ms' 'x' 'y' 0.1'
'set string 'ti2
'set strsiz 0.2'
'draw string 'x+0.01' 'y-0.05' 'c1
say c1 'hour' 'lat' 'lon' 'hgt' 'ti
if (c1=5)
    prompt 'Press enter to see next batch'
    pull temp
    'c'
    'set lev 'level
    'set gxout contour'
    'set mproj scaled'
    'set mpdset mres'
    'set annot 0'
    'set background 1'
    'set xlopts 0'
    'set ylopts 0'
    'set line 0'
    'set grid on 5 0'
    'set background 1'
    'set map 15 1 1'
    'c'
    'set clevs 1 2'
    'set ccolor 3 2'
    'set clevs 1 2'
    'set ccols 17 18'
    'set gxout shaded'
    'd h'
    'draw title Date 'date2' file=test'tme'.ctl'
    c1=0
endif
c1=c1+1
endif
endif
prompt 'Press enter to see next time!'

```

```
    pull temp
    tme=tme+12
    'reinit'
endwhile
endif
endwhile
```

Appendix D: Turbulence Viewer Code

The below html and javascript code makes up the layer viewer. The first segment of this appendix lists the necessary directories and which files go in it and a brief description of the files if the actual code is not included. This is followed by the code that makes up the two main sections of the framed script.

DIRECTORY STRUCTURE (d=directory, otherwise file)

Levels (d)

Level100.htm – basic html containing the flight level associated with 100mb



Level700.htm – same as above except associated with 700mb

script_output (d)

12_level100.jpg – image file from 12 hour forecast at 100-150 mb layer



24_level750.jpg – image file from 24 hour forecast at 100-150 mb layer

Scrollbars (d)

Scrollbar_0.jpg – image of scrollbar with bar at top to “animate” scrollbar



Scrollbar_6.jpg – image of scrollbar with bar at bottom to “animate” scrollbar

Turb_files (d)

Bottom_half.htm – sets up bottom frames for 12 hour forecast, code below

Bottom_half_24.htm – similar to Bottom_half.htm for 24 hour forecast

buttons1.htm – engine that drives the layer viewer, code included below

buttons1_24.htm – similar to buttons1.htm for 24 hour forecast

layers.htm – sets up the layer frame with initial images

layers_24.htm – similar to layers.htm for 24 hour forecast

levels.htm – puts initial flight levels in flight level frame

TopTitle.htm – puts a title in the title frame

TopTitle_24.htm – similar to TopTitle.htm for 24 hour forecast

Turb_Layer_Viewer.htm – main html code that sets up a top and bottom frame

Turb_Layer_Viewer_24.html – similar to Turb_Layer_Viewer.htm for 24 hour forecast

Bottom_half.htm

```
<html>
```

```
<frameset cols="75%,12%,13%">
```

```
<frame src="layers.htm" name="layers" scrolling="yes">
```

```
<frame src="levels.htm" name="levels" scrolling="no">
```

```
<frame src="buttons1.htm" name="buttons" scrolling="auto">
```



```

    } else if (UD ==2) {
        changeIty=-1*CHANGEAMT;
        temp4=eval(temp4-1);
    } else if (UD == 3) {
        changeItx=-1*CHANGEAMT;
        temp4=eval(temp4-1);
    } else {
        changeItx=CHANGEAMT;
        temp4=eval(temp4+1);
    }
    if (temp4 < 0) {
        temp4=0;
    }
    if (temp4 > SCROLLMAX) {
        temp4=SCROLLMAX;
    }
    document.myForm.ScrollVal.value=temp4;
    temp=eval(document.myForm.newY.value);
    temp2=temp+changeIty;
    temp=eval(document.myForm.newX.value);
    temp3=temp+changeItx;
    if (temp2 < 0) {
        temp2=0;
    }
    if (temp3 < 0) {
        temp3=0;
    }
    document.myForm.newY.value=temp2;
    document.myForm.newX.value=temp3;
    for (var i=0; i< FRAMESPERPAGE; i++) {
        parent.layers.frames[i].scroll(temp3,temp2);
    }
    document.UDScroll.src=UDScrollImage[temp4].src;
}

```

```

function ScrollJump(xy)
{
// Jumps to that point on the scrollbar
    var changepoint=xy*CHANGEAMT;
    for (var i=0; i<FRAMESPERPAGE; i++) {
        parent.layers.frames[i].scroll(0,changepoint);
    }
    document.UDScroll.src=UDScrollImage[xy].src;
    document.myForm.ScrollVal.value=xy;
    document.myForm.newY.value=changepoint;
}

```

```

}

function MajorScroll(ud)
{
    var nexttone=parseInt(document.myForm.UDVal.value);
    if (ud == 1) {
        nexttone--;
    } else {
        nexttone++;
    }
    if (nexttone < 0) {
        nexttone = 0;
    }
    if (nexttone > (LEVELMAX-3)) {
        nexttone = LEVELMAX-3;
    }
    document.myForm.UDVal.value=nexttone;
    var bullet;
    for (var i=0; i < FRAMESPERPAGE; i++) {
        bullet=i+nexttone;
        with (parent.layers.frames[i].document) {
            open()
            writeln("");
            close();
        }
        with (parent.levels.frames[i].document) {
            open()
            writeln("<html><font
size=6><center><B>FL"+labels[bullet]+</B></center></font></html>");
            close();
        }

        parent.layers.frames[i].scroll(0,parseInt(document.myForm.newY.value,10));
    }
}

</script>

<form name="myForm" method=post>
    <input type=hidden name="newY" value=0>
    <input type=hidden name="newX" value=0>
    <input type=hidden name="ScrollVal" value=0>
    <input type=hidden name="UDVal" value=0>
</form>

```

```

<map name="NSmap">
  <area shape="rect" coords="0,0,15,14" onClick="ScrollIt(2);">
  <area shape="rect" coords="0,15,15,33" onClick="ScrollJump(0);">
  <area shape="rect" coords="0,34,15,53" onClick="ScrollJump(1);">
  <area shape="rect" coords="0,54,15,73" onClick="ScrollJump(2);">
  <area shape="rect" coords="0,74,15,93" onClick="ScrollJump(3);">
  <area shape="rect" coords="0,94,15,113" onClick="ScrollJump(4);">
  <area shape="rect" coords="0,114,15,132" onClick="ScrollJump(5);">
  <area shape="rect" coords="0,133,15,151" onClick="ScrollJump(6);">
  <area shape="rect" coords="0,152,15,166" onClick="ScrollIt(1);">
</map>


<center>
<b>Click on scrollbar to move up and down inside the layers</b>
<br><br><br><br><br>
  <form name="myForm2" method=post>
    <input type=button value=" UP " onClick="MajorScroll(1);">
    <br>
    <input type=button value="DOWN" onClick="MajorScroll(2);">
  </form>
<b>Click on buttons to move shift the viewable layers up or down</b>

</html>

```

Appendix E: FORTRAN Code Used in Computing Indices

The below is the FORTRAN code used to compute the indices and save the data in the proper format. It consists of the functions called by a main program which simply reads in the model data files and saves the indices for display using GrADS.

```
MODULE KEmodule
```

```
CONTAINS
```

```
! Subroutines used with KE.f90 to compute indices version 3
```

```
!-----  
SUBROUTINE Haversine(lat1,lat2,lon1,lon2,dist)
```

```
! Uses the Haversine method to compute distance
```

```
IMPLICIT NONE
```

```
! Declarations passed from main program
```

```
REAL, INTENT(IN):: lat1,lat2,lon1,lon2
```

```
REAL, INTENT(OUT):: dist
```

```
! Locally used declarations
```

```
REAL a,c,dlon,dlat,ER,PI,lat1r,lat2r,lon1r,lon2r
```

```
! Executable portion
```

```
ER=6371000.0
```

```
PI=4*atan(1.)
```

```
! Converts degrees to radians
```

```
lat1r=lat1*PI/180
```

```
lat2r=lat2*PI/180
```

```
lon1r=lon1*PI/180
```

```
lon2r=lon2*PI/180
```

```
! Computes the difference in latitude/longitude between points
```

```
dlat=lat2r-lat1r
```

```
dlon=lon2r-lon1r
```

```

! Calculates the distance
a=(sin(dlat/2))**2+cos(lat1r)*cos(lat2r)*(sin(dlon/2))**2
c=2*atan(sqrt(a)/sqrt(1-a))
dist=ER*c

```

```

END SUBROUTINE Haversine

```

```

!-----

```

```

!-----

```

```

SUBROUTINE Ellrod2
(U,V,H,BLAT,ELAT,BLON,ELON,usx,usy,LVLS,DY,BXSZ,xsz,KE,HU,KEmax)

```

```

! This subroutine calculates the Ellrod-2 index and returns a
! final KE value. Unlike AFWA, this index takes the average
! of two levels and converts that to a "layer" value

```

```

IMPLICIT NONE

```

```

! Declare calling parameters
REAL, INTENT(IN):: U(:, :, :), V(:, :, :), H(:, :, :), DY, BXSZ
INTEGER, INTENT(IN):: BLAT, ELAT, BLON, ELON, LVLS, usx, usy, xsz
REAL, INTENT(INOUT):: KE(:, :, :), HU(:, :, :), KEmax(:, :)

```

```

! Locally stored variables
INTEGER flag,i,j,k,a,b,lat,lon,dx,x,y,z
REAL kemx,dudx,dudy,dvdx,dvdy,dudz,dvdz,dst,dsh,def,div,vws,dist
REAL, ALLOCATABLE:: H2(:, :, :)

```

```

! Allocates a temporary array for storing the level heights
x=SIZE(H,1)
y=SIZE(H,2)
z=SIZE(H,3)
ALLOCATE(H2(x,y,z))

```

```

! Calculates the Ellrod-2 index for every grid point
! Calculates for an extra row/column to allow PIREP interpolation to work on border
flag=0.0

```

```

DO k=2,LVLS

```

```

  a=1

```

```

  DO j=BLAT,(ELAT-1),-1

```

```

    b=1

```

```

    lat=91-j

```

```

    DO i=BLON,(ELON+1)

```

```

      IF (xsz .EQ. 181) THEN

```

```

        ! To account for two different

```

```

lon=i-181          ! file sizes
ELSE
  IF (i .GT. 181) THEN
    lon=i-361
  ELSE
    lon=i-1
  END IF
END IF
CALL Haversine((1.0*lat),(1.0*lat),(1.0*lon),(1.0*lon+BXSZ),dist)
dx=2*dist
dudx=(U((i+1),j,k)-U((i-1),j,k))/dx
dvdx=(V((i+1),j,k)-V((i-1),j,k))/dx
dudy=(U(i,(j+1),k)-U(i,(j-1),k))/DY
dvdy=(V(i,(j+1),k)-V(i,(j-1),k))/DY
dudz=(U(i,j,(k+1))-U(i,j,(k-1)))/(H(i,j,(k+1))-H(i,j,(k-1)))
dvdz=(V(i,j,(k+1))-V(i,j,(k-1)))/(H(i,j,(k+1))-H(i,j,(k-1)))
dst=dudx-dvdy
dsh=dvdx+dudy
def=SQRT(dsh*dsh+dst*dst)
div=dudx+dvdy
vws=SQRT(dudz*dudz+dvdz*dvdz)
KE(b,a,(k-1))=vws*(def-div)*10**7
IF (KE(b,a,(k-1)) < 0.0) THEN
  KE(b,a,(k-1))=0.0
END IF
b=b+1
END DO
a=a+1
END DO
END DO

PRINT *, 'Averaging height and KE values to match MWF output levels'
DO k=2,LVLS
  kemx=0.0
  DO b=1,usx
    DO a=1,usy
      IF (KE(b,a,(k-1)) .GT. kemx) THEN
        kemx=KE(b,a,(k-1))
      END IF
      IF (KE(b,a,(k-1)) .GT. KEmax(b,a)) THEN
        KEmax(b,a)=KE(b,a,(k-1))
      END IF
      HU(b,a,(k-1))=(H(b,a,k)+H(b,a,(k+1)))/2
    END DO
  END DO
END DO

```



```

    PRINT *, ' Level ',(k-1), ' of ',(LVLS-1), ' done...max=',kemx
END DO

```

```

END SUBROUTINE Ellrod2

```

```

!-----

```

```

!-----

```

```

SUBROUTINE Mwfm_grid
(BLAT,ELAT,BLON,ELON,xsz,mwlat,mwlon,mwflux,raylat,raylon,rayflux,MWSZ,LV
LS,endv1,endv2,MW1,MW2,MW1max,MW2max)

```

```

! Lays the MWFM data onto a 1x1 degree grid
! Uses the maximum value in a box as the value of a grid point
! To prevent smoothing of the data

```

```

IMPLICIT NONE

```

```

! Declares calling parameters

```

```

INTEGER, INTENT(IN):: BLAT,ELAT,BLON,ELON,LVLS,xsz,endv1(:),endv2(:)
REAL, INTENT(IN):: mwlat(:,),mwlon(:,),mwflux(:,)
REAL, INTENT(IN):: raylat(:,),raylon(:,),rayflux(:,)
REAL, INTENT(IN):: MWSZ
REAL, INTENT(OUT):: MW1(:,,:), MW2(:,,:),MW1max(:,),MW2max(:,)

```

```

! Local variables

```

```

INTEGER i,j,k,a,b,lat,lon,q2

```

```

! Execution portion

```

```

PRINT *, 'Converting MWFM raw data into gridded format'

```

```

DO k=1,(LVLS-1)

```

```

    a=1

```

```

    DO j=BLAT,ELAT,-1

```

```

        b=1

```

```

        lat=91-j

```

```

        DO i=BLON,ELON

```

```

            IF (xsz .EQ. 181) THEN

```

```

                lon=i-181

```

```

                ! To account for two different
                ! file sizes

```

```

            ELSE

```

```

                IF (i .GT. 181) THEN

```

```

                    lon=i-361

```

```

                ELSE

```

```

                    lon=i-1

```

```

                END IF

```

```

            END IF

```

```

IF ((a .EQ. 1) .AND. (b .EQ. 1) .AND. (k .EQ. 1)) THEN
  PRINT *, 'Bottom left lat,Lon: ',lat,',',lon
END IF

! V1.1 gridding
MW1(b,a,k)=0.0
DO q2=1, endv1(k)
  IF ((mwlat(q2,k) .GE. (lat-MWSZ)) .AND. (mwlat(q2,k) .LE. (lat+MWSZ)))
THEN
  IF ((mwlon(q2,k) .GE. (lon-MWSZ)) .AND. (mwlon(q2,k) .LE.
(lon+MWSZ))) THEN
    IF (MW1(b,a,k) .LT. mwflux(q2,k)) THEN
      MW1(b,a,k)=mwflux(q2,k)
    END IF
  END IF
END IF
END DO
IF (MW1(b,a,k) .GT. MW1max(b,a)) THEN
  MW1max(b,a)=MW1(b,a,k)
END IF

! V2.1 gridding
MW2(b,a,k)=0.0
DO q2=1, endv2(k)
  IF ((raylat(q2,k) .GE. (lat-MWSZ)) .AND. (raylat(q2,k) .LE. (lat+MWSZ)))
THEN
  IF ((raylon(q2,k) .GE. (lon-MWSZ)) .AND. (raylon(q2,k) .LE.
(lon+MWSZ))) THEN
    IF (MW2(b,a,k) .LT. rayflux(q2,k)) THEN
      MW2(b,a,k)=rayflux(q2,k)
    END IF
  END IF
END IF
END DO
IF (MW2(b,a,k) .GT. MW2max(b,a)) THEN
  MW2max(b,a)=MW2(b,a,k)
END IF
b=b+1
END DO
a=a+1
END DO
PRINT *, 'Level ',k,' of ',(LVLS-1),' Done!'
END DO

END SUBROUTINE Mwfm_grid

```

```

!-----
!-----
SUBROUTINE
PR_int(MPR,BLAT,BLON,LVLS,METHOD,IX,endv1,endv2,BXSZ2,KEmax,MW1max
,MW2max,KE,HU,MW1,MW2,H)

! Interpolates INDICES to PIREPS
! Uses nearest neighbor for Ellrod-2 index
! Uses one of two methods for MWFM
!     METHOD=1. Uses nearest neighbor
!     METHOD=2. Uses closest point within a small box

IMPLICIT NONE

! Declarations passed from main program
INTEGER, INTENT(IN):: MPR,BLAT,BLON,LVLS,METHOD,IX,endv1(:),endv2(:)
REAL, INTENT(IN):: BXSZ2,KEmax(:,,:),MW1max(:,,:),MW2max(:,:)
REAL, INTENT(IN):: KE(:,,:),HU(:,,:),MW1(:,,:),MW2(:,,:),H(:,,:)

! Declarations used by this program
INTEGER
i,numpir,Pyear(MPR),Pmon(MPR),Pday(MPR),Phr(MPR),Palt(MPR),Pturb(MPR)
INTEGER elvlo,elvlu,mlvlu,mlvlo,gridx,gridy,ni,nj,k,xsz,ysz
REAL eoff,Plat(MPR),Plon(MPR),Plvl,lon2,lat2,dist
REAL
Pke_1,Pmw1_1,Pmw2_1,d1,d2,d3,d4,ew1,ew2,mww1,mww2,wtot,t1,t2,m1d,m2d,Pke_m,
Pmw1_m,Pmw2_m
CHARACTER (LEN=2) fcst_hr
CHARACTER (LEN=10) outfn

! Executable
xsz=SIZE(MW1,1)
ysz=SIZE(MW1,2)
PRINT *, 'Reading the PIREP data file'
101 FORMAT(F5.2,X,F7.2,X,I4,X,I2,X,I2,X,I2,X,I5,X,I1)
OPEN (UNIT=20, FILE='../PIREPS/PIREP.txt', STATUS='old')
  i=1
  eoff=2.3
  990 IF (eoff.EQ. 11.11) GOTO 991
    READ (20,101) Plat(i), Plon(i), Pyear(i), Pmon(i), Pday(i), Phr(i), Palt(i), Pturb(i)
    eoff=Plat(i)
    i=i+1
  GO TO 990
991 CLOSE(20)

```

```

numpir=i-2
PRINT *, 'There are ', numpir, ' PIREPS available in the 3 hour window'

PRINT *, 'Storing the indice values for each PIREP over the ', (LVLS-1), ' levels.'
PRINT *, 'Approximate Level height range ', HU(1,1,1), ' to ', HU(1,1,(LVLS-1)), ' meters.'
OPEN (UNIT=11, FILE='outfile.tmp', STATUS='old')
  READ(11,*) fcst_hr
CLOSE (11)
outfn='out//fcst_hr//'.txt'
OPEN (UNIT=20, FILE=outfn, STATUS='replace')
102
FORMAT(A2,X,F6.2,X,F7.2,X,I2,I2,2X,I2,3X,I5,3X,I1,4X,F6.2,X,F8.5,X,F8.5,X,F8.5,
X,F8.1,X,F8.5,X,F8.1)
103
FORMAT(A2,X,F6.2,X,F7.2,X,I2,I2,2X,I2,3X,I5,3X,I1,4X,F6.2,X,F8.5,X,F8.5,2X,F6.2,
X,F8.5,X,F8.5)
104
FORMAT(A2,X,F6.2,X,F7.2,X,I2,I2,2X,I2,3X,I5,3X,I1,4X,F6.2,X,F8.5,X,F8.5,X,F8.5,
X,F8.1)
105
FORMAT(A2,X,F6.2,X,F7.2,X,I2,I2,2X,I2,3X,I5,3X,I1,4X,F6.2,X,F8.5,X,F8.5,19X,F8.
5,X,F8.1)
PRINT *, 'PIREP REPORT'
PRINT *, 'Hr Lat   Lon  Date Hour Hght Turb   KE   MW1   MW2'

DO i=1,numpir
  ! Converts feet to meters
  Plvl=1.0*Palt(i)/3.28084
  lon2=1.0*FLOOR(Plon(i))
  lat2=1.0*FLOOR(Plat(i))
  gridx=nint(lon2)
  gridy=nint(lat2)
  IF (IX .EQ. 181) THEN
    ni=gridx+141
  ELSE
    IF (gridx .LT. 0) THEN
      ni=gridx+362-BLON
    ELSE
      ni=gridx+2-BLON
    END IF
  END IF
  IF (gridy .LT. 0) THEN
    gridy=gridy-1
  END IF
  nj=gridy-90+BLAT

```

```

DO k=2,LVLS
  IF ((H(ni,nj,k) .GT. Plvl) .OR. (k .EQ. LVLS)) THEN
    IF (k .eq. LVLS) THEN
      elvlu=LVLS-1
      elvlo=LVLS-1
      mlvlu=elvlu
      mlvlo=elvlo
      ew1=1.0
      mww1=1.0
      GOTO 805
    ELSE IF (K .EQ. 2) THEN
      elvlu=1
      elvlo=1
      mlvlu=elvlu
      mlvlo=elvlo
      ew1=1.0
      mww1=1.0
      GOTO 805
    ELSE
      elvlu=k-1
      elvlo=k
      mlvlu=elvlu
      mlvlo=elvlo
      ew1=1-(Plvl-H(ni,nj,elvlu))/(H(ni,nj,elvlo)-H(ni,nj,elvlu))
      mww1=1-(Plvl-HU(ni,nj,mlvlu))/(HU(ni,nj,mlvlo)-HU(ni,nj,mlvlu))
      GOTO 805
    END IF
  ELSE IF (H(ni,nj,k) .EQ. Plvl) THEN
    elvlu=k-1
    elvlo=k-1
    mlvlu=elvlu
    mlvlo=elvlo
    ew1=1.0
    mww1=1.0
    PRINT *, 'PIREP on one level'
    GOTO 805
  END IF
END DO
805 IF (ew1 .LT. 0.5) THEN
  elvlu=elvlu
ELSE
  elvlu=elvlo
END IF
IF (mww1 .LT. 0.5) THEN
  mlvlu=mlvlu

```

```

ELSE
  mlvlu=mlvlo
END IF
CALL Haversine(Plat(i),lat2,Plon(i),lon2,dist)
d1=dist
CALL Haversine(Plat(i),lat2,Plon(i),(lon2+1),dist)
d2=dist
CALL Haversine(Plat(i),(lat2+1),Plon(i),lon2,dist)
d3=dist
CALL Haversine(Plat(i),(lat2+1),Plon(i),(lon2+1),dist)
d4=dist
IF (d1 .EQ. MIN(d1,d2,d3,d4)) THEN
  ni=ni
  nj=nj
ELSE IF (d2 .EQ. MIN(d1,d2,d3,d4)) THEN
  ni=ni+1
  nj=nj
ELSE IF (d3 .EQ. MIN(d1,d2,d3,d4)) THEN
  ni=ni
  nj=nj+1
ELSE
  ni=ni+1
  nj=nj+1
END IF
Pke_l=KE(ni,nj,elvlu)
Pke_m=KEmax(ni,nj)
Pmw1_l=MW1(ni,nj,mlvlu)
Pmw1_m=MW1max(ni,nj)
Pmw2_l=MW2(ni,nj,mlvlu)
Pmw2_m=MW2max(ni,nj)

WRITE (20,103)
fcst_hr,Plat(i),Plon(i),Pmon(i),Pday(i),Phr(i),Palt(i),Pturb(i),Pke_l,Pmw1_l,Pmw2_l,Pke_
m,Pmw1_m,Pmw2_m
WRITE (*,103)
fcst_hr,Plat(i),Plon(i),Pmon(i),Pday(i),Phr(i),Palt(i),Pturb(i),Pke_l,Pmw1_l,Pmw2_l,Pke_
m,Pmw1_m,Pmw2_m
END DO
CLOSE (20)

END SUBROUTINE PR_int
!-----
!-----

```

```

SUBROUTINE
Comp_make(COMPMETHOD,usx,usy,LVLS,KEL,KEM,KES,MW1L,MW1M,MW1S,
MW2L,MW2M,MW2S,KE,MW1,MW2,KEmax,MW1max,MW2max,HF)

! Makes the composite index grid point values
IMPLICIT NONE

! Declarations passed from main program
INTEGER, INTENT(IN):: COMPMETHOD,usx,usy,LVLS
REAL, INTENT(IN):: KEL,KEM,KES,MW1L,MW1M,MW1S,MW2L,MW2M,MW2S
REAL, INTENT(IN)::
KE(:, :, :),MW1(:, :, :),MW2(:, :, :),KEmax(:, :),MW1max(:, :),MW2max(:, :)
REAL, INTENT(OUT):: HF(:, :)

! Declarations used by this program
INTEGER i,j,k
PRINT *, 'Comp_make',KEL,KEM,KES,MW1L,MW1M,MW1S,MW2L,MW2M,MW2S
HF(1:usx,1:usy)=0.0
IF (COMPMETHOD .EQ. 1) THEN
  PRINT *, 'Method 1'
  DO k=2,(LVLS-2)
    DO i=1,usx
      DO j=1,usy
        IF (HF(i,j) .LT. 1.0) THEN
          IF ((KE(i,j,(k-1)) .GE. KEL) .AND. (KE(i,j,k) .GE. KEL) .AND.
(KE(i,j,(k+1)) .GE. KEL)) THEN
            HF(i,j)=1.0
          END IF
          IF ((MW1(i,j,(k-1)) .GE. MW1L) .AND. (MW1(i,j,k) .GE. MW1L) .AND.
(MW1(i,j,(k+1)) .GE. MW1L)) THEN
            HF(i,j)=1.0
          END IF
          IF ((MW2(i,j,(k-1)) .GE. MW2L) .AND. (MW2(i,j,k) .GE. MW2L) .AND.
(MW2(i,j,(k+1)) .GE. MW2L)) THEN
            HF(i,j)=1.0
          END IF
        END IF
      END IF
    END IF
  END IF
  IF (HF(i,j) .LT. 2.0) THEN
    IF ((KE(i,j,(k-1)) .GE. KEM) .AND. (KE(i,j,k) .GE. KEM) .AND.
(KE(i,j,(k+1)) .GE. KEM)) THEN
      HF(i,j)=2.0
    END IF
  END IF
  IF ((MW1(i,j,(k-1)) .GE. MW1M) .AND. (MW1(i,j,k) .GE. MW1M) .AND.
(MW1(i,j,(k+1)) .GE. MW1M)) THEN
    HF(i,j)=2.0
  END IF

```

```

        END IF
        IF ((MW2(i,j,(k-1)) .GE. MW2M) .AND. (MW2(i,j,k) .GE. MW2M) .AND.
(MW2(i,j,(k+1)) .GE. MW2M)) THEN
            HF(i,j)=2.0
        END IF
    END IF
    IF (HF(i,j) .LT. 3.0) THEN
        IF ((KE(i,j,(k-1)) .GE. KES) .AND. (KE(i,j,k) .GE. KES) .AND.
(KE(i,j,(k+1)) .GE. KES)) THEN
            HF(i,j)=3.0
        END IF
        IF ((MW1(i,j,(k-1)) .GE. MW1S) .AND. (MW1(i,j,k) .GE. MW1S) .AND.
(MW1(i,j,(k+1)) .GE. MW1S)) THEN
            HF(i,j)=3.0
        END IF
        IF ((MW2(i,j,(k-1)) .GE. MW2S) .AND. (MW2(i,j,k) .GE. MW2S) .AND.
(MW2(i,j,(k+1)) .GE. MW2S)) THEN
            HF(i,j)=3.0
        END IF
    END IF
END DO
END DO
END DO
ELSE
    PRINT *, 'Method 2'
    Do i=1,usx
        DO j=1,usy
            HF(i,j)=0.0
            IF (KEmax(i,j) .GE. KEL) THEN
                HF(i,j)=1.0
            END IF
            IF (KEmax(i,j) .GE. KEM) THEN
                HF(i,j)=2.0
            END IF
            IF (KEmax(i,j) .GE. KES) THEN
                HF(i,j)=3.0
            END IF
        END DO
    END DO
END IF
END SUBROUTINE Comp_make
!-----
END MODULE KEmodule

```


Bibliography

- Air Force Manual 15-124, 2001: Meteorological Codes. [Available online at: [http://www.e-publishing.af.mil/.](http://www.e-publishing.af.mil/)]
- Air Force Manual 15-129, 2001: Aerospace Weather Operations – Processes and Procedures. [Available online at: [http://www.e-publishing.af.mil/.](http://www.e-publishing.af.mil/)]
- Allen, M. S., 2003: Evaluation of the Mountain Wave Forecast Model's Stratospheric Turbulence Simulations. Thesis, Air Force Institute of Technology, Wright-Patterson Air Force Base, OH, 70 pp.
- Bacmeister, J. T., 1993: Mountain wave drag in the stratosphere and mesosphere inferred from observed winds and a simple mountain wave parameterization scheme. *Journal of Atmospheric Science*, **50**, 377-399.
- Bacmeister, J. T., P. A. Newman, B. L. Gary, and K. R. Chan, 1994: An algorithm for forecasting mountain wave-related turbulence in the stratosphere. *Weather and Forecasting*, **9**, 241-253.
- Brown, R., 1973: New Indices to Locate Clear-Air Turbulence. *Meteorological Magazine*, **102**, 347-361.
- Brown, B.G., J. L. Mahoney, J. Henderson, T. Kane, R. Bullock, and J. E. Hart, 2000: The Turbulence Algorithm Comparison Exercise: Statistical Comparison and Results. Preprints, 9th Conference on Aviation, Range, and Aerospace Meteorology, Orlando, FL, 11-15 September 2000, American Meteorological Society, 466-471.
- Brown, B. G. and G.S. Young, 2000: Verification of Icing and Turbulence Forecasts: Why Some Verification Statistics can't be Computed Using PIREPS. Preprints, 9th Conference on Aviation, Range, and Aerospace Meteorology, Orlando, FL, 11-15 September 2000, American Meteorological Society, 393-398.
- Chandler, C.L., 1987: Turbulence Forecasting. *NASA, Langley Research Center Atmospheric Turbulence Relative to Aviation, Missile and Space Programs*, 137-154.
- Colson, D., and H. A. Panofsky, 1965: An Index of CLEAR-AIR Turbulence. *Quarterly Journal of the Royal Meteorological Society*, **91**, 507-513.
- Drazin, P. G. and W. H. Reid, 1981: *Hydrodynamic Stability*. Cambridge, 527pp.
- Dutton, M. J. O., 1980: Probability Forecasts of Clear-Air Turbulence based on Numerical Model Output, *Meteorological Magazine*, **108**, 293-306.

- Eckermann, S. D., D. Broutman, and J. T. Bacmeister, 2000: Aircraft Encounters with Mountain Wave Induced Clear-Air Turbulence: Hindcasts and Operational Forecasts using an Improved Global Model. Preprints, *9th Conference on Aviation, Range, and Aerospace Meteorology*, Orlando, FL, 11-15 September, American Meteorological Society, 456-459.
- Eckermann, S. D., A. Dornbrack, S. Vosper, and K. Carslaw, 2001: Mesoscale Forecasting of the Stratosphere During SOLVE-THESEO 2000, Unpublished Paper, 7-13.
- Ellrod, G. P., 1989: An Index for CLEAR-AIR Turbulence based on Horizontal Deformation and Vertical Wind Shear. Preprints, *3rd International Conference on the Aviation Weather System*, Anaheim, CA 30 Jan-3 Feb, American Meteorological Society, 339-344.
- Ellrod, G. P. and D. I. Knapp, 1991: An Objective Clear-Air Turbulence Forecasting Technique: Verification and Operational Use. *Weather and Forecasting*, **7**, 150-167.
- Endlich, R. M., 1964: The Mesoscale Structure of some Regions of Clear-Air Turbulence. *Monthly Weather Review*, **92**, 261-276.
- FAA, cited 2003: Federal Aviation Administration: Regulations and Policies. [Available online at: <http://www/ncsa.uiuc.edu/General/Internet/WWW/HTMLPrimer.html>.]
- Grid Analysis and Display System (GrADS), 2003: Documentation. [Available online at: <http://grads.iges.org/grads>]
- Holton, J. R., 1992: *An Introduction to Dynamic Meteorology*. Academic Press, 511 pp.
- Hopkins, R. H., 1977: Forecasting Techniques of Clear-Air Turbulence Including That Associated with Mountain Waves, *Technical Note No. 155*, World Meteorological Organization, 31 pp.
- Kronebach, G. W., 1964. An Automated Procedure for Forecasting Clear-Air Turbulence, *Journal of Applied Meteorology*, **3**, 119-125.
- Marks, C. J., and S. D. Eckermann, 1995: A Three-Dimensional Nonhydrostatic Ray Tracing Model for Gravity Waves: Formulation and Preliminary Results for the Middle Atmosphere. *Journal of Atmospheric Science*, **52**, 1959-1984.
- Marroquin, A., 1985: An Integrated Algorithm to Forecast CAT from Gravity Wave Breaking, Upper Fronts and Other Atmospheric Deformation Regions. Preprints,

- 6th Conference on Aviation Weather Systems, Dallas, TX, American Meteorological Society, 509-514.
- Marroquin, A., 1998: An Advanced Algorithm to Diagnose Atmospheric Turbulence using Numerical Model Output. Preprints, 16th Conference on Weather Analysis and Forecasting, Phoenix, AZ, 11-16 January, American Meteorological Society.
- Montgomery, D. C., and G. C. Runger, 2003: *Applied Statistics and Probability for Engineers, 3rd Edition*. John Wiley and Sons, Inc., 706pp.
- National Center for Environmental Prediction (NCEP), 2003: The GFS Atmospheric Model description. [Available online at <http://www.emc.ncep.noaa.gov/gmb/moorthi/gam.html>]
- Naval Research Laboratory (NRL), 2003: MWFM: Model Description. [Available online at <http://uap-www.nrl.navy.mil/dynamics/html/mwfmusa.html>.]
- Neiman, P. J., and J. A. Shaw, 2003: Coronas and Iridescence in Mountain Wave Clouds over Northeastern Colorado. *Bulletin of the American Meteorological Society*, **84**, 1373-1386.
- Petterson, S., 1956: *Weather Analysis and Forecasting, Vol 1. Motion and Motion Systems*. 2nd edition, McGraw-Hill, 428pp.
- Ray, P. S., 1986: *Mesoscale Meteorology and Forecasting*. American Meteorological Society, Boston, 793pp.
- Schaefer, J. T., 1990: The Critical Skill Index as an Indicator of Warning Skill. *Weather and Forecasting.*, **5**, 570-575.
- Sharman, R., B. Brown, and S. Dettling, 2000: Preliminary Results of the NCAR Integrated Turbulence Forecasting Algorithm (ITFA) to Forecast CAT. Preprints, 9th Conference on Aviation, Range, and Aerospace Meteorology, Orlando, FL, 11-15 September, American Meteorological Society, 460-465.
- Sinclair, P. C. and Kuhn, P. M., 1991: *Infrared Detection of High Altitude Clear Air Turbulence*, NOARL Technical Note 205, 49pp.
- Sinnott, R. W., 1984: Virtues of the Haversine. *Sky and Telescope*, **68**, 159.
- Stephenson, D.B., 2000: Use of the "Odds Ratio" for Diagnosing Forecast Skill. *Weather and Forecasting*, **15**, 221-232.
- Thorpe, S.A., 1969: Experiments on the Stability of Stratified Shear Flows. *Radio Science*, **4**, 1327-1331.

Wallace, J. M. and Hobbs, P. V., 1977: *Atmospheric Science: An Introductory Survey*. Academic Press, 467pp.

Wilks, D.S., 1995: *Statistical Methods in the Atmospheric Sciences*. Academic Press, 467pp.

WMO-No. 306, 1995: Manual on Codes, 492pp.

WMO-No. 958, 2003: Aircraft Meteorological Data Relay (AMDAR) Reference Manual, 80pp.

Glossary

AFCCC	Air Force Combat Climatology Center
AFGWC	Air Force Global Weather Central (currently AFWA)
AFWA	Air Force Weather Agency (formerly AFGWC)
AVAR	Automated vertical accelerometer
AVN	Aviation model
CAT	Clear-air Turbulence
CONUS	Continental United States
CVG	Convergence
CSI	Critical Skill Index
DEF	Deformation shear to include shearing and stretching deformation
DSH	Shearing deformation
DST	Stretching deformation
FAA	Federal Aviation Administration
FAR	False alarm rate
FL	Flight Level
FTP	file transfer protocol
FORTRAN	Formula Translation programming language
GFS	Global Forecast System
GrADS	Gridded Analysis and Display System
GRIB	Gridded Binary format
GSM	Global spectral model
GSS	Gilbert Skill Score
HiCAT	High altitude clear-air turbulence software
HIRAS	High-Resolution Analysis System
HSS	Heidke Skill Score
IDL	Interactive Data Language
ITFA	Integrated turbulence forecast algorithm
JPEG	Joint Photographic Experts Group
MB	MegaBytes
MOG	Moderate or greater
MSL	Mean sea level
MWFM	Mountain wave forecast model
NCAR	National Center for Atmospheric Research
NCEP	National Center for Environmental Prediction
NGM	Nested grid model
NMC	National Meteorological Center
NRL	Naval Research Laboratory
OPS II	Operational Production System version II
OWS	Operational Weather Squadron
PIREP	Pilot report
POD	Probability of detection
POD _n	Probability of detection of regions without turbulence

PODy	Probability of detection of regions with turbulence
RAOB	Rawinsonde observation program
Ri	Richardson number
TI_1	Ellrod index 1
TI_2	Ellrod index 2
TSS	True skill score
USAF	United States Air Force
VE	Volume efficiency
VWS	Vertical wind shear
WMO	World Meteorological Organization

Vita

Capt Brian Belson was born in Georgia in 1972. Upon completion of high school in 1990, he enlisted in the United States Navy and received training to become a Nuclear Reactor Operator. After completing training, he was awarded an ROTC scholarship and graduated from Tulane University in 1997 with a Bachelor of Science degree in Computer Science. After a brief stint at Undergraduate Pilot Training, he opted for the Basic Meteorology Program at Florida State University in Tallahassee, Florida.

His first assignment was Wing Weather Officer for the 15th Operational Support Squadron, Hickam AFB, Hawaii. In 2000, Capt Belson was assigned to the Joint Typhoon Warning Center as the Satellite Systems Officer at Pearl Harbor, Hawaii. In 2001, he was reassigned to be Regional Weather Operations Flight Commander at the 17th Operational Weather Squadron, Hickam AFB, Hawaii. Most recently, he was selected to attend the Air Force Institute of Technology in 2002. Capt Belson is married and has one daughter.

REPORT DOCUMENTATION PAGE			<i>Form Approved</i> <i>OMB No. 074-0188</i>		
<p>The public reporting burden for this collection of information is estimated to average 1 hour per response, including the time for reviewing instructions, searching existing data sources, gathering and maintaining the data needed, and completing and reviewing the collection of information. Send comments regarding this burden estimate or any other aspect of the collection of information, including suggestions for reducing this burden to Department of Defense, Washington Headquarters Services, Directorate for Information Operations and Reports (0704-0188), 1215 Jefferson Davis Highway, Suite 1204, Arlington, VA 22202-4302. Respondents should be aware that notwithstanding any other provision of law, no person shall be subject to a penalty for failing to comply with a collection of information if it does not display a currently valid OMB control number.</p> <p>PLEASE DO NOT RETURN YOUR FORM TO THE ABOVE ADDRESS.</p>					
1. REPORT DATE (DD-MM-YYYY) 05-03-2004		2. REPORT TYPE Master's Thesis		3. DATES COVERED (From - To) Jun 2003 - Mar 2004	
4. TITLE AND SUBTITLE AN AUTOMATED METHOD OF PREDICTING CLEAR-AIR TURBULENCE			5a. CONTRACT NUMBER		
			5b. GRANT NUMBER		
			5c. PROGRAM ELEMENT NUMBER		
6. AUTHOR(S) Belson, Brian L., Captain, USAF			5d. PROJECT NUMBER		
			5e. TASK NUMBER		
			5f. WORK UNIT NUMBER		
7. PERFORMING ORGANIZATION NAMES(S) AND ADDRESS(S) Air Force Institute of Technology Graduate School of Engineering and Management (AFIT/ENP) 2950 Hobson Way, Bldg 640 WPAFB OH 45433-7765			8. PERFORMING ORGANIZATION REPORT NUMBER AFIT/GM/ENP/04-02		
9. SPONSORING/MONITORING AGENCY NAME(S) AND ADDRESS(ES) 15 th Operational Weather Squadron 102 W. Losey St., Room 205 Scott AFB, IL 62225-5206			10. SPONSOR/MONITOR'S ACRONYM(S)		
			11. SPONSOR/MONITOR'S REPORT NUMBER(S)		
12. DISTRIBUTION/AVAILABILITY STATEMENT APPROVED FOR PUBLIC RELEASE; DISTRIBUTION UNLIMITED.					
13. SUPPLEMENTARY NOTES					
14. ABSTRACT Clear-air turbulence (CAT) prediction is vitally important to military aviation and the successful completion of Department of Defense (DoD) operations such as air to air refueling and new national defensive weapon systems such as directed energy platforms. The unique mission requirements of military aircraft often require strict avoidance of turbulent regions. Traditionally, weather forecasters have found it difficult to accurately predict CAT. In order to forecast regions where CAT might occur, forecasters must first determine the location of breaking waves caused by either Kelvin-Helmholtz instabilities or topographically forced internal gravity waves (mountain waves) in the atmosphere. The United States Air Force (USAF) 15 th Operational Weather Squadron (15th OWS) requested an updated method of predicting CAT and this request was ranked as one of the highest priority research needs by the HQ USAF Director of Weather, Deputy Chief of Staff for Air and Space Operations. A new method of forecasting turbulence was developed in this work and the operational model was delivered to the 15 th OWS for immediate inclusion into their operations. This method combines output from the Knapp-Ellrod index and the Naval Research Laboratory's Mountain Wave Forecast Model (MWFM) onto a single chart. Displaying these tools together allows forecasters to view both causes of CAT simultaneously. Furthermore, a new visualization tool is developed that allows a forecaster to view several layers at the same time as well as a composite chart to greatly reduce the time required to produce turbulence charts by OWS forecasting centers worldwide. Tests of forecast accuracy, as determined by pilot reports (PIREPS), between charts currently produced by USAF OWSs and this new method were compared, with the new method producing far superior forecast results. This method revolutionizes the way USAF OWSs produce turbulence charts to help the Air Force satisfy each of its core competencies; especially information superiority, rapid global mobility, and precision engagement.					
15. SUBJECT TERMS Clear-Air Turbulence, CAT, Turbulence, Aviation Hazards, Kelvin-Helmholtz Instabilities, Mountain Waves					
16. SECURITY CLASSIFICATION OF:		17. LIMITATION OF ABSTRACT	18. NUMBER OF PAGES	19a. NAME OF RESPONSIBLE PERSON	
REPORT	ABSTRACT			THIS PAGE	Lt Col Michael K. Walters, ENP
U	U	U	112	19b. TELEPHONE NUMBER (Include area code) (937) 255-3636, ext 4681	